

# Assessing the near surface sensitivity of SCIAMACHY atmospheric CO<sub>2</sub> retrieved using (FSI) WFM-DOAS

M. P. Barkley<sup>1,\*</sup>, P. S. Monks<sup>2</sup>, A. J. Hewitt<sup>1</sup>, T. Machida<sup>3</sup>, A. Desai<sup>4</sup>, N. Vinnichenko<sup>5,†</sup>, T. Nakazawa<sup>6</sup>, M. Yu Arshinov<sup>7</sup>, N. Fedoseev<sup>8</sup>, and T. Watai<sup>9</sup>

<sup>1</sup>EOS, Department of Physics and Astronomy, University of Leicester, UK

<sup>2</sup>Department of Chemistry, University of Leicester, UK

<sup>3</sup>National Institute for Environmental Studies, Tsukuba, Japan

<sup>4</sup>National Centre for Atmospheric Research, Boulder, CO, USA

<sup>5</sup>Central Aerological Observatory, Dolgoprudny, Russia

<sup>6</sup>Tohoku University, Sendai, Japan

<sup>7</sup>Institute of Atmospheric Optics, Tomsk, Russia

<sup>8</sup>Permafrost Institute, Yakutsk, Russia

<sup>9</sup>Global Environmental Forum, Tsukuba, Japan

\* now at: Institute for Atmospheric and Environmental Science, School of GeoSciences, University of Edinburgh, UK

† deceased 2006

Received: 30 January 2007 – Published in Atmos. Chem. Phys. Discuss.: 21 February 2007

Revised: 25 April 2007 – Accepted: 29 June 2007 – Published: 9 July 2007

**Abstract.** Satellite observations of atmospheric CO<sub>2</sub> offer the potential to identify regional carbon surface sources and sinks and to investigate carbon cycle processes. The extent to which satellite measurements are useful however, depends on the near surface sensitivity of the chosen sensor. In this paper, the capability of the SCIAMACHY instrument on board ENVISAT, to observe lower tropospheric and surface CO<sub>2</sub> variability is examined. To achieve this, atmospheric CO<sub>2</sub> retrieved from SCIAMACHY near infrared (NIR) spectral measurements, using the Full Spectral Initiation (FSI) WFM-DOAS algorithm, is compared to in-situ aircraft observations over Siberia and additionally to tower and surface CO<sub>2</sub> data over Mongolia, Europe and North America.

Preliminary validation of daily averaged SCIAMACHY/FSI CO<sub>2</sub> against ground based Fourier Transform Spectrometer (FTS) column measurements made at Park Falls, reveal a negative bias of about –2.0% for collocated measurements within ±1.0° of the site. However, at this spatial threshold SCIAMACHY can only capture the variability of the FTS observations at monthly timescales. To observe day to day variability of the FTS observations, the collocation limits must be increased. Furthermore, comparisons to in-situ CO<sub>2</sub> observations demonstrate that SCIAMACHY is capable of observing a seasonal signal

that is representative of lower tropospheric variability on (at least) monthly timescales. Out of seventeen time series comparisons, eleven have correlation coefficients of 0.7 or more, and have similar seasonal cycle amplitudes. Additional evidence of the near surface sensitivity of SCIAMACHY, is provided through the significant correlation of FSI derived CO<sub>2</sub> with MODIS vegetation indices at over twenty selected locations in the United States. The SCIAMACHY/MODIS comparison reveals that at many of the sites, the amount of CO<sub>2</sub> variability is coincident with the amount of vegetation activity. The presented analysis suggests that SCIAMACHY has the potential to detect CO<sub>2</sub> variability within the lowermost troposphere arising from the activity of the terrestrial biosphere.

## 1 Introduction

Although water vapour is by far the dominant greenhouse gas, contributing to 60% of the greenhouse effect, its short residence time (~10 days) means that it is considered as a natural feedback, rather than forcing agent (Kiehl and Trenberth, 1997). Of the anthropogenic greenhouse gases, carbon dioxide (CO<sub>2</sub>) generates the largest forcing and is considered the principal species with methane (CH<sub>4</sub>) the next most important. Whereas at any given instant the mean global energy

Correspondence to: P. S. Monks  
(psm7@le.ac.uk)

balance is governed by water vapour and clouds, over long time scales (i.e. decades and longer) it is predominately regulated by CO<sub>2</sub>. Over the last 200 years there has been a dramatic ~30% rise in atmospheric CO<sub>2</sub> owing primarily to the burning of fossil fuels and deforestation. This significant increase is likely to have a serious impact on the carbon cycle and climate, as present concentrations are now greater than at any other time in the last half a million years (Siegenthaler et al., 2005).

Two important carbon cycle sinks which absorb CO<sub>2</sub> from the atmosphere, and keep levels lower than otherwise, are the terrestrial biosphere and the ocean. The terrestrial biosphere draws down CO<sub>2</sub> through the creation and accumulation of plant biomass, whereas CO<sub>2</sub> that diffuses across the atmosphere-ocean interface is mixed to deep waters by the solubility, biological and carbonates pumps. However, there is much uncertainty about where, and how, this uptake occurs. As global carbon emissions show no sign of slowing, the variability and efficiency of the terrestrial and oceanic sinks will play an important role in shaping the Earth's future climate. Present estimates of the global carbon cycle fluxes, provided by inverse modelling (e.g. Rödenbeck et al., 2003; Patra et al., 2006), are restricted by the sparse distribution and limited number of available measurements (Gurney et al., 2002). The greater spatial and temporal coverage offered by satellite observations, if of sufficient (~1%) precision, coupled with inverse models can help identify surface sources and sinks and reduce flux uncertainties (O'Brien and Rayner, 2002; Houweling et al., 2004; Miller et al., 2007). Satellite observations therefore offer a unique ability to investigate the dynamics of the carbon cycle. However, one of the most important aspects of satellite CO<sub>2</sub> measurements is the question of near-surface sensitivity i.e. can the instrument observe CO<sub>2</sub> variability within the lower troposphere, where the signatures of surface fluxes occur?

Thermal infrared sounders, such as AIRS, have limited sensitivity to surface CO<sub>2</sub> as the light that the sensor detects originates from the mid-upper troposphere (Engelen and McNally, 2005; Tiwari et al., 2006). In contrast, NIR instruments such as SCIAMACHY (the only current operational NIR sensor) or the future OCO and GOSAT missions, are sensitive to the lower troposphere since they detect light that is reflected from the Earth's surface i.e. which has traversed the atmospheric path completely. Previous work by Buchwitz et al. (2005a,b, 2006), Houweling et al. (2005) and Barkley et al. (2006a,b,c) have shown that CO<sub>2</sub> measurements from SCIAMACHY are possible with a precision that is approaching the 1% threshold requirement for inverse flux modelling (O'Brien and Rayner, 2002) and with an estimated accuracy of a couple of percent.

In this paper, SCIAMACHY CO<sub>2</sub>, retrieved using the (FSI) WFM-DOAS algorithm (Barkley et al., 2006a,b,c), is initially validated against ground based Fourier Transform Spectrometer (FTS) column measurements and then compared to in situ aircraft, tower and surface CO<sub>2</sub> observations

to assess if SCIAMACHY is able to detect changes in surface CO<sub>2</sub> concentrations. Although SCIAMACHY measures the CO<sub>2</sub> column integral, in situ observations of atmospheric CO<sub>2</sub> mixing ratios made at the surface or from aircraft can provide a useful comparison data set. However, care must be taken when performing any analysis. In situ observations occur at a specific location, time and altitude whereas typically the SCIAMACHY CO<sub>2</sub> corresponds to a column VMR which is often given as a monthly gridded product (to improve the precision). Thus, a comparison of the magnitudes, phasing and the general behaviour of the seasonal cycle are often the only features that can be examined with any meaning. Thus, validation of SCIAMACHY CO<sub>2</sub> using surface data will, for the most part, be performed using monthly average time series although comparisons to spatially and temporally collocated aircraft measurements over Siberia are demonstrated.

Furthermore, in the second part of this paper, the North American region is selected for a case study. The spatial distributions over this scene for 2003 and 2004 are examined whilst additionally vegetation proxy data, taken from the MODIS instrument, is compared to SCIAMACHY CO<sub>2</sub> at over twenty locations within the U.S. to assess if there is any observable correlation between terrestrial vegetation activity and atmospheric CO<sub>2</sub> concentrations. Any significant correlation between SCIAMACHY derived CO<sub>2</sub> and vegetation at specific locations will be further evidence of near surface sensitivity.

This paper is structured as follows. Section 2 contains a brief description of SCIAMACHY whilst Sect. 3 gives an overview of the FSI retrieval algorithm. Validation of SCIAMACHY/FSI CO<sub>2</sub> against ground based FTS measurements is discussed in Sect. 4 with the detailed comparisons to aircraft, tower and surface measurements performed in Sect. 5. The case study over North America is documented in Sect. 6 with overall conclusions given in Sect. 7.

## 2 The SCIAMACHY instrument

The SCanning Imaging Absorption spectroMeter for Atmospheric CHartography (SCIAMACHY) instrument is a passive UV-VIS-NIR hyper-spectral spectrometer designed to investigate atmospheric composition and processes (Bovensmann et al., 1999; Gottwald et al., 2006). It was launched onboard the ENVISAT satellite, in March 2002, into a near polar sun-synchronous orbit, from which it can observe the Earth from three viewing geometries: nadir, limb and lunar/solar occultation. The instrument measures sunlight that is reflected from the surface or scattered by the atmosphere, covering the spectral range 240–2380 nm (non-continuously) using eight separate grating spectrometers (or channels), with moderate spectral resolution 0.2–1.4 nm. For the majority of its orbit SCIAMACHY make measurements in an alternating limb and nadir sequence. The total columns of

CO<sub>2</sub> are derived from nadir observations in the NIR, using a small micro-window within channel six, centered on the CO<sub>2</sub> band at 1.57 μm. For channel 6, the nominal size of each pixel within the 960×30 km<sup>2</sup> (across×along track) swath is 60×30 km<sup>2</sup> which corresponds to an integration time of 0.25 s. Full longitudinal (global) coverage is achieved at the Equator within 6 days.

### 3 Full Spectral Initiation (FSI) WFM-DOAS

The Full Spectral Initiation (FSI) WFM-DOAS retrieval algorithm, discussed in detail in Barkley et al. (2006a,b,c), has been developed specifically to retrieve CO<sub>2</sub> from space using SCIAMACHY NIR spectral measurements. It is a development of the WFM-DOAS algorithm first introduced by Buchwitz et al. (2000) whereby the trace gas vertical column density (VCD) can be retrieved through a linear least squares fit of the logarithm of a model reference spectrum  $I_i^{\text{ref}}$  and its derivatives, plus a quadratic polynomial  $P_i(a_m)$  (i.e.  $m=2$ ), to the logarithm of the measured sun normalized intensity  $I_i^{\text{meas}}$ .

$$\left\| \ln I_i^{\text{meas}}(\mathbf{V}^t) - \left[ \ln I_i^{\text{ref}}(\bar{\mathbf{V}}) + \sum_j \frac{\partial \ln I_i^{\text{ref}}}{\partial \bar{V}_j} \cdot (\hat{V}_j - \bar{V}_j) + P_i(a_m) \right] \right\|^2 \equiv \|\text{RES}_i\|^2 \rightarrow \min \text{ w.r.t } \hat{V}_j \text{ \& } a_m \quad (1)$$

where the subscript  $i$  refers to each detector pixel of centre wavelength  $\lambda_i$ . The polynomial  $P_i(a_m)$  (which has coefficients  $a_0$ ,  $a_1$  and  $a_2$ ) is included to account for the spectral continuum and broadband scattering. The true, model and retrieved vertical columns are represented by  $\mathbf{V}^t=(V_{\text{CO}_2}^t, V_{\text{H}_2\text{O}}^t, V_{\text{Temp}}^t)$ ,  $\bar{\mathbf{V}}=(\bar{V}_{\text{CO}_2}, \bar{V}_{\text{H}_2\text{O}}, \bar{V}_{\text{Temp}})$  and  $\hat{V}_j$ , respectively (where  $j$  refers to the variables CO<sub>2</sub>, H<sub>2</sub>O and temperature). Each derivative represents the change in radiance at the top of the atmosphere as a function of a relative scaling of the corresponding trace gas or temperature profile. It should be noted that  $V_{\text{Temp}}$  is not a vertical column but rather a scaling factor applied to the vertical temperature profile. The fit parameters are the trace gas columns  $\hat{V}_{\text{CO}_2}$  and  $\hat{V}_{\text{H}_2\text{O}}$ , the temperature scaling factor  $\hat{V}_{\text{Temp}}$  and the polynomial coefficients  $a_m$ . The error, associated with each of the fit parameters, is given by Eq. (2) where  $(\mathbf{C}_\mathbf{x})_{jj}$  refers to the  $j$ th diagonal element from the least squares fit covariance matrix,  $\text{RES}_i$  is the fit residual,  $m$  is the number of spectral points within the fitting window and  $n$  is the number of fit parameters.

$$\sigma_{\hat{V}_j} = \sqrt{\frac{(\mathbf{C}_\mathbf{x})_{jj} \times \sum_i \text{RES}_i^2}{(m-n)}} \quad (2)$$

The main focus of the FSI algorithm is the inclusion of a priori data within the retrieval in order to minimize the error

associated with the retrieved CO<sub>2</sub> column. The FSI algorithm differs from current implementations of WFM-DOAS (e.g. Buchwitz et al., 2005b, 2006) in that rather than using a look-up table approach, it generates a reference spectrum for each individual SCIAMACHY observation. Each model spectrum is created using the radiative transfer model SCIATRAN (Rožanov et al., 2002), which includes the latest version of the HITRAN molecular spectroscopic database (Rothman et al., 2005), from several sources of a priori data including:

- A CO<sub>2</sub> vertical profile is selected from a specially prepared climatology (Remedios et al., 2006)
- Temperature, pressure and water vapour profiles, derived from operational 6 hourly ECMWF data (1.125°×1.125° grid)
- An approximate value for the surface albedo is inferred using the mean radiance (within the fitting window) and the solar zenith angle of the SCIAMACHY observation
- Maritime, rural and urban aerosol scenarios are implemented over the oceans, land and urban areas respectively using the LOWTRAN aerosol model (Kneizys et al., 1996).

As the line by line calculation of radiances is computationally expensive, the FSI algorithm is not implemented on an iterative basis. Instead, each reference spectrum is only used as the best possible linearization point for the retrieval. The potential error from not performing any iterations is kept to a minimum, since the a priori data generate model spectra that closely approximate SCIAMACHY measurements. In order to avoid possible instrumental issues, that hinder retrievals when using the NIR channels (e.g. Gloudemans et al., 2005), the raw SCIAMACHY spectra (v5.04) are calibrated in-house. Corrections for the orbit specific dark current and detector non-linearity (Kleipool, 2003a,b) are applied. Furthermore, a solar spectrum with improved calibration is also used (courtesy of ESA). All SCIAMACHY observations are cloud screened prior to retrieval processing, using the cloud detection method devised by Krijger et al. (2005), with cloud contaminated pixels flagged and disregarded. Back-scans along with observations that have solar zenith angles greater than 75° are also not processed. To produce a CO<sub>2</sub> vertical column volume mixing ratio (VMR) each retrieved VCD is normalized using the input ECMWF surface pressure. To clean the data from potential biases arising from aerosols or undetected (and partial) cloud contamination only VMRs that have retrieval errors less than 5% and that are within the range 340–400 ppmv are used. Any CO<sub>2</sub> column VMRs lying outside this range are classed as failed retrievals.

**Table 1.** Summary of the Park Falls FTS and SCIAMACHY comparison, showing the collocation limits, the number of daily match ups  $N_c$ , the mean bias  $B$  and its  $1\sigma$  standard deviation, the mean column VMRs,  $M_{\text{FTS}}$  and  $M_{\text{SCIA}}$  for the FTS and SCIAMACHY measurements respectively and their corresponding  $1\sigma$  standard deviations  $\sigma_{\text{FTS}}$  and  $\sigma_{\text{SCIA}}$ , and  $N_{\text{FSI}}$  which is the number of SCIAMACHY observations used in the calculation of  $M_{\text{SCIA}}$ . The correlation  $r$  between the daily means is given in the last column.

Collocation Limits (lon × lat)	$N_c$ [–]	$B$ [%]	$\sigma_B$ [%]	$M_{\text{FTS}}$ [ppmv]	$\sigma_{\text{FTS}}$ [ppmv]	$M_{\text{SCIA}}$ [ppmv]	$\sigma_{\text{SCIA}}$ [ppmv]	$N_{\text{FSI}}$ [–]	$r$ [–]
0.5° × 0.5°	13	−3.1	2.6	374.4	2.4	362.8	10.8	4	0.54
1.0° × 1.0°	20	−2.1	2.3	374.5	2.1	366.7	9.3	10	0.36
2.0° × 2.0°	26	−1.6	1.8	374.3	2.7	368.2	7.7	24	0.49
3.0° × 3.0°	29	−1.5	1.6	374.5	2.7	369.1	7.8	40	0.73
4.0° × 4.0°	30	−1.3	1.6	374.4	2.7	369.5	7.5	55	0.71
5.0° × 5.0°	34	−1.1	1.4	374.4	2.6	370.2	6.8	69	0.71
10.0° × 10.0°	40	−0.9	1.3	374.4	2.8	371.0	6.2	208	0.68

**Table 2.** Summary of the simulated seasonal cycle amplitudes for the retrieved and true column VMRs,  $\hat{V}_{\text{CO}_2}$  and  $V_{\text{CO}_2}^t$  respectively, in comparison to the seasonal cycles at the surface and for different altitudes within the lower troposphere when using the CO<sub>2</sub> climatology (Remedios et al., 2006). A mean SCIAMACHY averaging kernel has been applied to the true vertical column  $V_{\text{CO}_2}^t$ .

Latitude	$V_{\text{CO}_2}^t$	$\hat{V}_{\text{CO}_2}$	Seasonal Cycle Amplitude [ppmv]						
			0 km	1 km	2 km	3 km	4 km	5 km	0–5 km
60–90° N	9.0	11.3	14.7	15.1	14.7	13.3	11.8	11.1	13.4
30–60° N	4.6	5.9	10.5	9.3	8.6	7.0	5.8	5.3	7.4
0–30° N	3.5	4.0	4.3	4.6	5.1	5.3	4.6	3.7	4.7
0–30° S	1.4	1.5	1.7	1.7	1.7	1.6	1.5	1.5	1.6
30–60° S	1.9	1.9	1.9	1.9	1.8	1.9	2.0	2.1	1.9
60–90° S	1.9	2.0	2.2	2.1	2.1	2.1	2.1	2.1	2.1

#### 4 Validation of SCIAMACHY CO<sub>2</sub> using Park Falls FTS measurements

Measurements of the CO<sub>2</sub> column integral by ground based Fourier Transform Spectrometers (FTS) provide the most useful means of validating NIR satellite CO<sub>2</sub> columns (e.g. Dils et al., 2006). Previous validation of SCIAMACHY/FSI CO<sub>2</sub> to FTS CO<sub>2</sub> measurements, made at Egbert (Canada) revealed a negative bias of about −4% to the measured CO<sub>2</sub> concentration (Barkley et al., 2006c). However, the Egbert site is in the region of the large urban centre of Toronto and thus may suffer from local contamination. A more suitable location for satellite CO<sub>2</sub> validation is the Park Falls site located within northern Wisconsin, where existing surface and tower CO<sub>2</sub> measurements are already made (e.g. Bakwin and Tans, 1995). The FTS based at this site, which is part of the Total Carbon Column Observing Network (TCCON)<sup>1</sup>, has already been used to test the OCO retrieval algorithm using SCIAMACHY NIR measurements (Bösch et al., 2006). The site itself, is surrounded by boreal and wetland forests and relatively flat terrain.

In this paper, measurements of the CO<sub>2</sub> column made by Washenfelder et al. (2006) are used to further assess the accuracy of the FSI retrieved CO<sub>2</sub>. As the FTS measurement procedure is thoroughly documented in Washenfelder et al. (2006), only a brief outline of the experimental set-up is given here. The CO<sub>2</sub> columns are derived from solar absorption spectra recorded by a Bruker 125HR FTS housed within a steel shipping container, adjacent to the WLEF TV tower that is situated at the site. The FTS is fully automated with an active solar tracker directing light, from the centre of the solar disk, into the FTS instrument which has a 2.4 mrad field of view. Dual detectors InGasAs and Si-diode detectors then simultaneously record solar spectra over the interval 3800–15 500 cm<sup>−1</sup> at high resolution (0.014 cm<sup>−1</sup>) which is sufficient to resolve individual CO<sub>2</sub> lines. Simultaneous retrieval of the CO<sub>2</sub> column from two bands centred at 6228 cm<sup>−1</sup> and 6348 cm<sup>−1</sup> and of the O<sub>2</sub> column from the band at 7882 cm<sup>−1</sup> is achieved using the non-linear least squares spectral fitting (GFIT) algorithm developed at the Jet Propulsion Laboratory. The CO<sub>2</sub> dry column average is then calculated via CO<sub>2</sub>/O<sub>2</sub> × 0.2095. Under clear sky observations the measurement precision is 0.1%. Calibration against integrated aircraft profiles indicate a bias of approximately −2.0% but good correlation.

<sup>1</sup> See <http://www.tcon.caltech.edu>.

**Table 3.** Summary of aircraft and SCIAMACHY comparison over Siberia. All values within the table are computed using only coincidental aircraft and SCIAMACHY observations (i.e. when both measurements occur on the same day). The amplitude of the seasonal cycles (SCA) are shown for SCIAMACHY (denoted SCIA) and for the aircraft over its complete sampling altitude range. The correlation between the aircraft and SCIAMACHY CO<sub>2</sub> is also shown in the last column.

Location	Vegetation Type	Number of flights	Altitude Range [km]	SCA [ppmv]		Correlation [-]
				Aircraft	SCIA	
Novosibirsk	Forest	12	0.0–7.0	23.5	21.0	0.79
Surgut	Wetland	12	0.0–7.0	11.0	26.0	0.90
Yakutsk	Forest	20	0.0–3.0	25.0	17.5	0.72

To determine the accuracy of FSI retrieved CO<sub>2</sub>, daily averaged SCIAMACHY observations, denoted SCIA<sub>D</sub>, collocated within incremental longitude and latitude limits of the Park Falls site (see Table 1), were directly compared to the daily mean FTS CO<sub>2</sub> VMR, denoted PF<sub>D</sub>, if available. The bias of each SCIAMACHY CO<sub>2</sub> column with respect to the ground based measurement is then given by:

$$\text{Bias} = \left( \frac{\text{SCIA}_D - \text{PF}_D}{\text{PF}_D} \right) \times 100\% \quad (3)$$

with the mean bias  $B$ , then simply the average over all the SCIAMACHY/FTS match-ups. By applying both the SCIAMACHY/FSI and the FTS averaging kernels (Fig. 2) to the CO<sub>2</sub> climatology, it has been verified that differences in the CO<sub>2</sub> columns owing to the different sensitivities of each instrument are small:  $\sim 1\text{--}2$  ppmv.

As Table 1 shows, the bias to the FTS measurements is very dependent on the collocation boundary limits selected around the Park Falls site. At close proximity, i.e. within  $0.5^\circ \times 0.5^\circ$ , the mean bias is  $-3.1\%$  however the number of SCIAMACHY/FTS match-ups  $N_c$  is small and few SCIAMACHY observations, indicated by  $N_{\text{FSI}}$ , are used to calculate the daily mean. At very large collocation limits (e.g.  $10.0^\circ \times 10.0^\circ$ ) this bias is reduced to only  $-0.9\%$  owing both to the greater number of match-ups and the greater number of SCIAMACHY observations used to calculate SCIA<sub>D</sub>. Assuming the errors are random, the precision and accuracy of SCIAMACHY/FSI CO<sub>2</sub> should significantly improve by the averaging process. This is reflected in the scatter of the SCIAMACHY data, which is reduced as  $N_{\text{FSI}}$  increases. The negative bias that is found for each of the collocation limits is better than, but consistent with the negative 4.0% offset also observed at Egbert (Barkley et al., 2006c).

For SCIAMACHY observations occurring within  $1.0^\circ \times 1.0^\circ$  of Park Falls (which is the spatial resolution of monthly gridded FSI data) the bias is  $-2.1\%$  but the correlation between the SCIAMACHY and FTS daily means is quite low at 0.36. This implies that SCIAMACHY fails to capture the day to day variability of the FTS measurements. Only once the collocation boundaries are expanded to at least  $3.0^\circ \times 3.0^\circ$  (and above) does the correlation become

significant. However, if the  $1.0^\circ \times 1.0^\circ$  limits are again used but with both data sets assembled into monthly averages then the bias is  $-2.2\%$  but the correlation improves to 0.94 (which is not attributable to the a priori climatology, see e.g. Figs. 12 and 13). This means that to capture day to day variability around Park Falls (or any FTS site) a wider overpass criteria must be tolerated but to capture monthly variability collocation limits of  $1.0^\circ \times 1.0^\circ$  resolution are acceptable. Either way the bias is about  $-2.0\%$ .

## 5 Assessing the near surface sensitivity of SCIAMACHY

### 5.1 Model simulations

The SCIAMACHY/FSI averaging kernels peak in the planetary boundary layer indicating increased sensitivity to the lower atmosphere (Fig. 2). However, before comparisons between SCIAMACHY and in situ surface data are made, it is necessary to use model simulations to ascertain what one would expect SCIAMACHY to observe as compared to the seasonal signal within the lower troposphere. To achieve this, simulated retrievals were performed using spectra generated from CO<sub>2</sub> profiles taken from the newly prepared climatology (Remedios et al., 2006). This climatology consists of 12 monthly profiles for each  $30^\circ$  latitude band (see, e.g. Fig. 1 of Barkley et al., 2006a). Initially, a baseline reference spectrum was created using the U.S. Standard atmosphere with a uniform a priori CO<sub>2</sub> profile scaled to 370 ppmv. Then, in each retrieval simulation a “measurement” spectrum was created by inputting into SCIATRAN the climatological CO<sub>2</sub> profile (interpolated onto the U.S. Standard pressure scale) along with the U.S. Standard temperature and water vapour profile. The baseline spectrum was then used to perform a synthetic retrieval against each “measurement” with the retrieved column VMR compared to (a) the true column VMR of the input climatological CO<sub>2</sub> profile, calculated after the application of a SCIAMACHY averaging kernel, and (b) the mixing ratio of the profile at the surface and also at selected altitudes between 0–5 km. Whilst these simulations differ from the FSI approach, which is based on not using fixed a

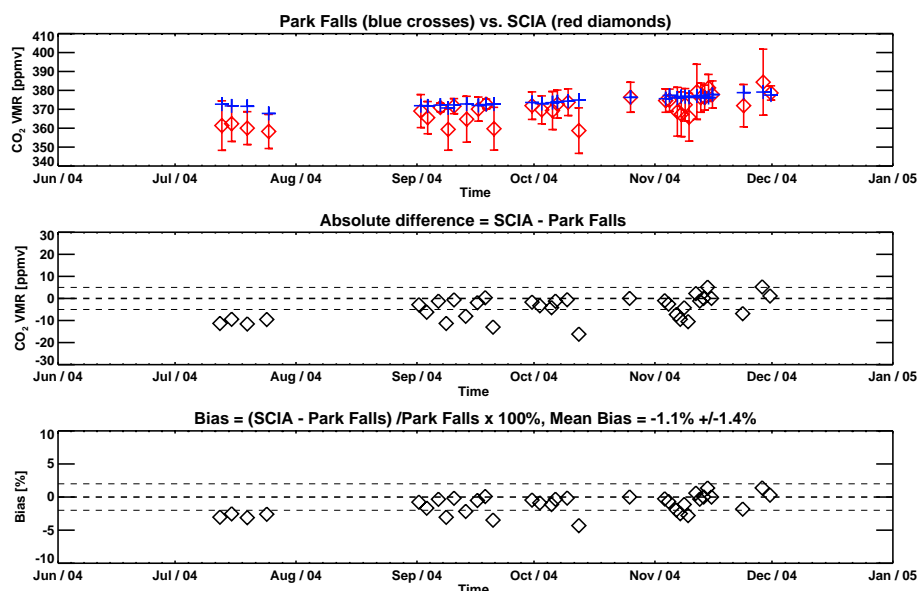


**Fig. 1.** Top Panel: The daily mean FTS CO<sub>2</sub> column measurements (blue crosses) with the corresponding daily average of all SCIAMACHY measurements (red diamonds) occurring within  $5.0^{\circ} \times 5.0^{\circ}$  of the Park Falls site together with its  $1\sigma$  standard deviation. Middle Panel: The absolute difference (SCIAMACHY minus FTS) between the satellite and ground based observations. The grey dashed lines indicate the  $\pm 5$  ppmv differences. Bottom Panel: The percentage bias of each SCIAMACHY observation with respect to the FTS measurements. The grey dashed lines indicate the  $\pm 2\%$  bias threshold.

priori data, they at least offer some indication of the difference between column and surface CO<sub>2</sub> mixing ratios.

The results of these simulations reveal that below  $30^{\circ}$  N the difference between the retrieved column VMR and those at the surface are very similar. In terms of absolute magnitudes, the column VMRs below  $30^{\circ}$  N are larger than those mixing ratios at the surface. Furthermore, the magnitude of the seasonal cycles and their phasing of their anomalies (not shown), are almost indistinguishable. Inter-hemispheric mixing in the upper troposphere, combined with weaker terrestrial uptake and release at the Southern Hemisphere surface, may both contribute to this finding.

Between  $60^{\circ}$ – $90^{\circ}$  N, the phasing between the surface and column VMRs also agrees well (Fig. 3). This is in spite of the fact the retrieved columns VMRs are lower in the spring months, relative to the mixing ratios at the surface and correspondingly higher in the summer months. Furthermore, within this latitude band, the seasonal cycle amplitude of the retrieved column VMRs (11.3 ppmv) is 2.3 ppmv higher than that of true column seasonal amplitude, whereas it is smaller when compared to the seasonal cycle observed at the surface, which is typically  $\sim 14$ – $15$  ppmv. The mean amplitude over 0–5 km is however is marginally larger than that of the retrieved column, 13.4 ppmv as compared to 11.3 ppmv. The over estimation of the true column amplitude within the simulated retrievals originates from the use of a single a priori CO<sub>2</sub> profile (Barkley et al., 2006a).

The seasonal cycles between  $30^{\circ}$ – $60^{\circ}$  N are similar to those at higher latitudes with the exception that the phasing of the

retrieved column VMRs slightly lags behind that at the surface at the spring/summer crossover of the CO<sub>2</sub> anomaly (i.e. when photosynthesis exceeds respiration). The delay of the crossover is coherent with the transport and vertical mixing of the seasonal signal from the surface to higher altitudes. Within this latitude range, the retrieved column VMR seasonal amplitude is 1.5 ppmv lower than that over 0–5 km but approximately 1 ppmv greater than the true column signal.

Thus, on the basis of these simulations, if one assumes that monthly averaged surface data is adequately representative of well mixed CO<sub>2</sub> below 5 km then, at mid to high northern latitudes, SCIAMACHY should see a seasonal signal smaller than that at the surface but which is in turn larger than that of the true seasonal amplitude of the column integral. Moreover, the phasing at high northern latitudes is expected to be consistent with that at the surface whilst at mid-latitudes a slight shift is more likely. In the Southern Hemisphere, the seasonal cycles amplitudes of the column VMRs should be of the same order of those at the surface with approximately the same phasing.

## 5.2 Comparison to aircraft CO<sub>2</sub> over Siberia

In this section, SCIAMACHY CO<sub>2</sub> column VMRs are compared to in-situ volume mixing ratios (denoted as vmrs to distinguish them from column measurements) measured from aircraft flights, made in 2003, over three Siberian locations: Novosibirsk, Surgut and Yakutsk (Fig. 4). The

CO<sub>2</sub> volume mixing ratios were determined using the air-sampling method as outlined in Machida et al. (2001). Over Novosibirsk and Surgut, chartered AN-30 and AN-24 aircraft were used respectively with samples taken by pressurizing air, fed into the cockpit through a drain pipe, into a 0.5 L Pyrex glass flask using a diaphragm pump. These systems were operated manually with the aircraft sampling at eight different altitudes between 0.0–7.0 km over both of these sites. Over Yakutsk, a smaller AN-2 aircraft was used which only sampled the altitudes 0.0–3.0 km during 2003. The CO<sub>2</sub> volume mixing ratios were derived from the flask samples to an accuracy of  $\sim 0.10$  ppmv, against standard gases, using a non-dispersive infrared analyzer (NDIR) at either Tohoku University, Japan (for Surgut measurements) or the National Institute for Environmental Studies (NIES), Japan (for Novosibirsk and Yakutsk measurements). To capture discrete events, SCIAMACHY observations occurring on the same day of each flight and collocated within  $\pm 10.0^\circ$  longitude and  $\pm 8.0^\circ$  latitude of each location, were averaged and compared to the mean of the aircraft measurements (convolved with a mean SCIAMACHY averaging kernel) over all sampling altitudes.

Over Yakutsk, the agreement between the aircraft CO<sub>2</sub> vmrs and the column VMRs measured by SCIAMACHY is poor (Fig. 5). However, the aircraft observations agree with SCIAMACHY on the timing and approximate magnitude of the minimum CO<sub>2</sub> at the end of July. The average difference between SCIAMACHY CO<sub>2</sub> and the mean aircraft CO<sub>2</sub> (over all altitudes) is typically less than 4% with the smallest difference occurring in July. The CO<sub>2</sub> anomalies, that is each measurement minus the mean of its data set, show similar behaviour with the best agreement being between the middle of May to the beginning of July when a significant amount of CO<sub>2</sub> uptake occurs. That said, the minimum of the aircraft anomaly dips lower than that of SCIAMACHY though the size of the return, between July and October, is approximately the same (8.7 ppmv for SCIAMACHY and 10.7 ppmv for the aircraft observations). The amplitude of the seasonal signal observed by the aircraft varies considerably with altitude and has a mean of 25.0 ppmv which is noticeably larger than that detected by SCIAMACHY (17.5 ppmv). The correlation between SCIAMACHY and the mean of the aircraft data is 0.72.

Over Novosibirsk, the overall difference between the mean aircraft CO<sub>2</sub> and SCIAMACHY is smaller than at that found at Yakutsk, only approximately 2% with the correlation 0.77 (Fig. 6). The aircraft data show an extremely large seasonal cycle amplitude in the lowest 1 km of  $>40$  ppmv which decreases with altitude. SCIAMACHY observes a smaller seasonal amplitude of 21.0 ppmv which is thus more comparable to the mean aircraft seasonal amplitude which is 23.5 ppmv. Examination of Fig. 6 reveals that in addition, the CO<sub>2</sub> anomalies measured over Novosibirsk show very good agreement between March–July. The change in the anomalies between October and December is also similar.

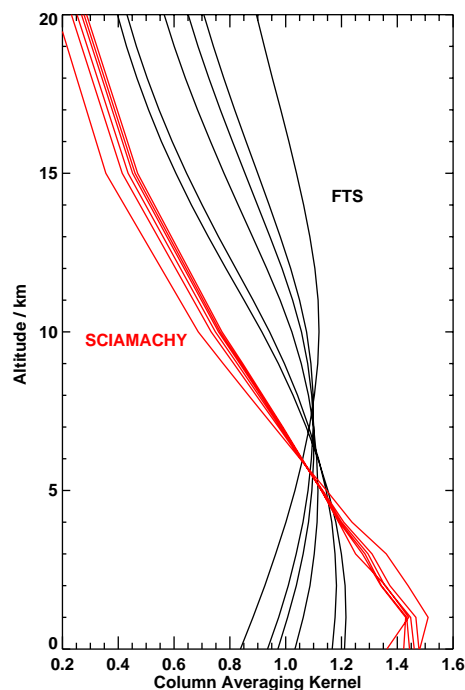


**Fig. 2.** Example averaging kernels, for various solar zenith angles (i.e. air masses), for SCIAMACHY (red line) and the FTS (black line) highlighting the different sensitivity of each instrument to the lower troposphere. The SCIAMACHY averaging kernels are calculated numerically (see, e.g. Barkley et al., 2006c).

Over Surgut there were only six coincidental SCIAMACHY observations (Fig. 7). Nevertheless, there is fairly good agreement between SCIAMACHY and the aircraft observations. The volume mixing ratios are of the same order of magnitude and the typical difference from mean aircraft observations is  $\sim 2\%$ . Unlike the measurements over Yakutsk or Novosibirsk, the amplitude of the seasonal cycle detected by SCIAMACHY (26.0 ppmv) is larger than the aircraft observations at any altitude or over any altitude range. At the surface, the seasonal amplitude is 19.9 ppmv which decreases rapidly with altitude to only 8.3 ppmv at 7.0 km. Thus, even though a quite strong seasonal cycle is evident at the surface it doesn't propagate to higher altitudes.

In summary, the FSI retrieved CO<sub>2</sub> shows fair agreement to the aircraft observations. Whilst the precision of the raw satellite columns is less than that of the monthly gridded data, the variation of atmospheric CO<sub>2</sub> over the selected Siberian locations is still captured by SCIAMACHY if large collocation limits are used.

### 5.3 Comparison to in-situ surface observations

#### 5.3.1 Europe and Mongolia

In addition to the aircraft comparison over Siberia, SCIAMACHY CO<sub>2</sub> has also been compared to ground based

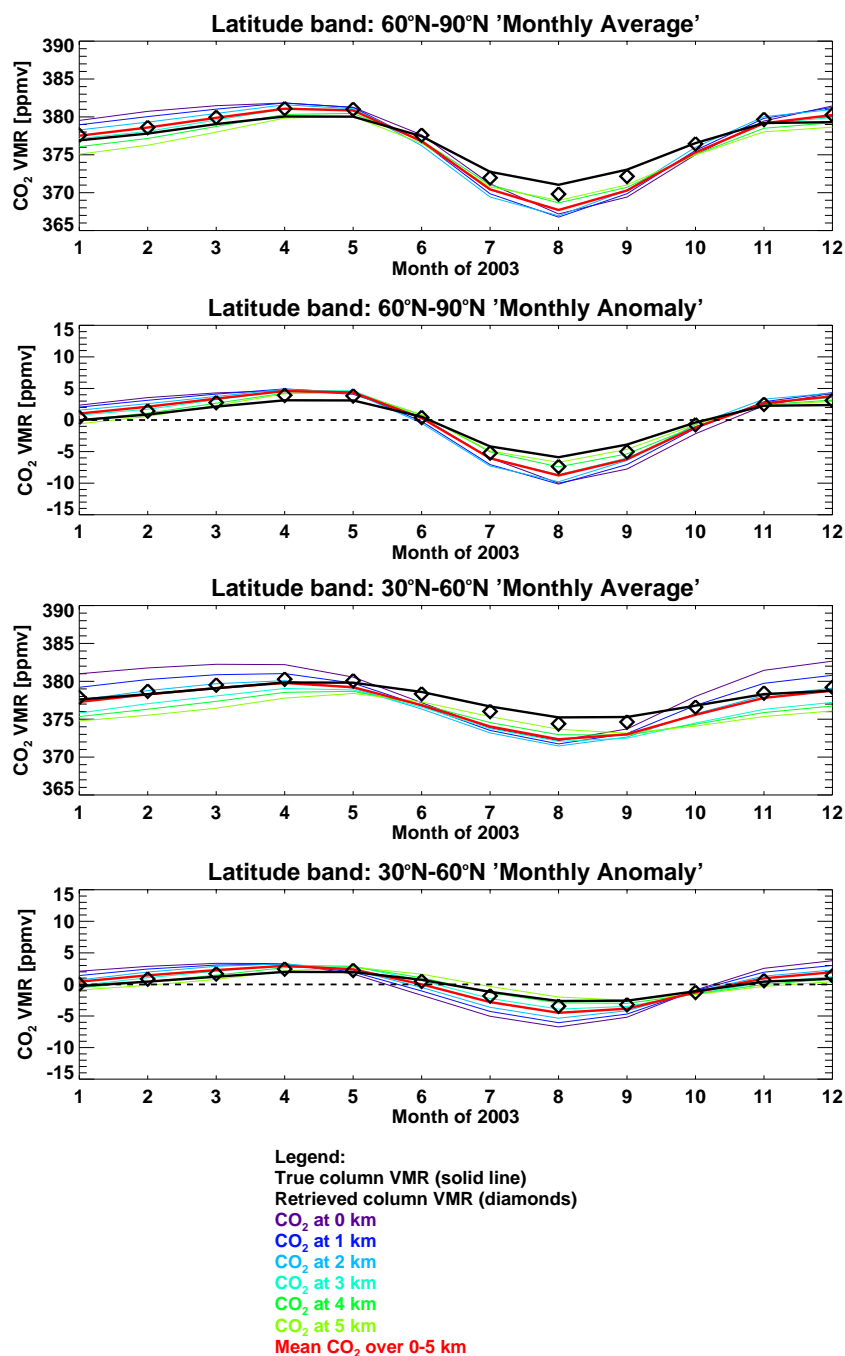


**Fig. 3.** Assessment of the near surface sensitivity of SCIAMACHY, for different latitude regions, using the 2003 CO<sub>2</sub> climatology. The plots show the retrieved and true column VMRs against CO<sub>2</sub> mixing ratios within the lower troposphere both in terms of absolute magnitudes and also the anomalies.

in-situ observations taken from the World Data Centre for Greenhouse Gases (WDCGG) network<sup>2</sup>. In this section this comparison is confined to Western Europe and to Mongolia (since SCIAMACHY retrievals over these region have already been processed for the TM3 model comparison doc-

umented in Barkley et al., 2006c). Within western Europe there were only five sampling sites which had CO<sub>2</sub> data for 2003 (shown in Fig. 8) whilst in Mongolia there was only a single station at Ulan Uul (47° N, 111° E). The CO<sub>2</sub> volume mixing ratios are measured, on a continuous or weekly basis, at these locations using NDIR analyzers. In this analysis, the monthly averages of the ground based observations have

<sup>2</sup>Downloadable from <http://gaw.kishou.go.jp/wdcgg.html>

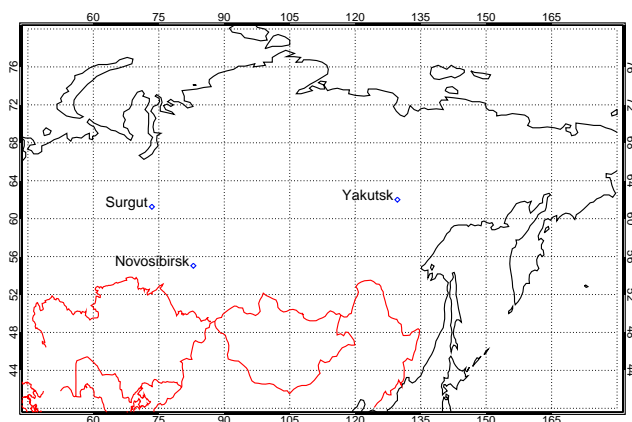


**Fig. 4.** The locations of the aircraft flights over Siberia during 2003: Novosibirsk (55.03° N, 82.19° E), Surgut (61.25° N, 73.41° E) and Yakutsk (62.00° N, 129.66° E).

been used, since the ability of SCIAMACHY to detect seasonal variations is being assessed. For this reason, the selection criteria for collocated satellite observations was based on using monthly ( $1^\circ \times 1^\circ$ ) gridded SCIAMACHY data, with the average taken of all grid points lying within  $\pm 3.5^\circ$  latitude and  $\pm 5.0^\circ$  longitude of each site. These collocation limits were chosen as a compromise between giving the most number of satellite match ups against proximity to the sampling location. The only exception was for the station at Ulaan Uul, which lies within the Gobi Desert. In this case, the monthly average of the whole scene was used, since the region is only  $8.0^\circ \times 18.0^\circ$  wide in the zonal and meridional directions.

Inspection of the time series of the ground based and SCIAMACHY measurements reveals that the in-situ observations are always about 2–4% larger than those observed from space (see Figs. 9 and 10). By only considering the CO<sub>2</sub> anomalies against one another this offset, for the most part, can be effectively removed. Thus, only a comparison between the CO<sub>2</sub> anomalies is feasible.

Of all the sampling sites, the Ulaan Uul anomaly agrees best with the column VMRs measured by SCIAMACHY. The correlation is 0.95 with the phasing and amplitude of the seasonal cycle matching exceptionally well. More importantly the seasonal cycle that SCIAMACHY observes does not simply follow the input a priori column VMRs (as indicated by the green lines in Figs. 9). In addition to Ulaan Uul, there is also excellent agreement at Deuselbach and Schauinsland which have correlation coefficients of 0.90 and 0.83, respectively. At Deuselbach, there is especially good agreement between SCIAMACHY and the surface anomalies during March–July. Furthermore, over both of these sites SCIAMACHY detects a seasonal cycle amplitude which is approximately the same as that at the surface (Table 4). These locations, which are close to one another, both show a small peak in August. Unfortunately, there aren't SCIAMACHY retrievals available for this month, due to instru-

**Table 4.** Summary of the in-situ ground based comparison over western Europe, Mongolia and the U.S. The seasonal cycle amplitudes (SCA) are given for both the ground based (g-b) and SCIAMACHY (SCIA) observations. The correlation between the time series is also given. The average correlation using all locations is 0.7.

Location	SCA [ppmv]		Correlation [-]
	g-b	SCIA	
<b>Surface:</b>			
Deuselbach, Germany	15.9	17.7	0.90
Mace Head, Eire	11.1	15.3	0.72
Neuglobsow, Germany	17.6	22.7	0.62
Plateau Rosa, Italy	8.6	10.1	0.56
Schauinsland, Germany	13.4	13.7	0.83
Ulaan Uul, Mongolia	11.5	10.6	0.95
Park Falls, Wisconsin, USA	23.1	17.4	0.72
Niwot Ridge, Colorado, USA	9.6	9.4	0.91
Point Arena, California, USA	13.3	8.3	0.39
Wendover, Utah, USA	9.9	11.7	0.85
<b>Tower:</b>			
Argyle, Maine, USA	7.7	30.1	0.19
Park Falls, Wisconsin, USA	18.0	17.4	0.93
Moody, Texas, USA	10.2	9.0	0.50
Sylvania Tower, Michigan, USA	15.9	18.4	0.76

ment decontamination, to corroborate this event. Over Mace Head, Neuglobsow and Plateau Rosa the anomalies agree less well. However, the comparison at both Mace Head and Neuglobsow is hampered as there are fewer SCIAMACHY observations (i.e. surrounding grid points) over these stations. Mace Head is on the coast, thus a higher number of retrievals are discarded, whereas Neuglobsow sits on the eastern edge of the Western Europe scene. The lack of gridded observations to the east of Neuglobsow clearly affects the agreement between SCIAMACHY and the ground based data. Comprehensive sampling and symmetrical spatial averaging of the SCIAMACHY data around each surface site is therefore necessary to avoid the time series being distorted (or influenced) by for example, pollution events, that occur in only one direction relative to the chosen location. Furthermore, the Plateau Rosa station is also at a very high altitude ( $>3$  km) within the Italian Alps. The effect of the surface topography on the SCIAMACHY retrievals is therefore much greater. Nevertheless, the seasonal amplitude measured at this station is similar to that observed by SCIAMACHY. However, in the spring months there appears to be a noticeable phase shift, with the transition from positive to negative occurring about two and a half months earlier for the observed SCIAMACHY signal.

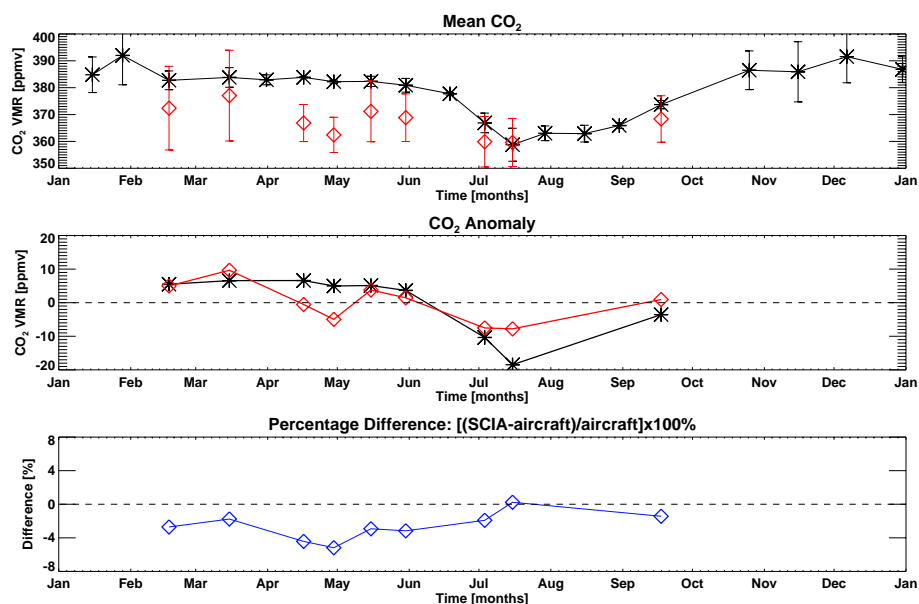


**Fig. 5.** The CO<sub>2</sub> time series over Yakutsk for SCIAMACHY (red) and aircraft (black). Top panel: The mean aircraft CO<sub>2</sub> mixing ratio (over all altitudes) and the SCIAMACHY VMRs. The error bars represent the 1σ uncertainty. Second panel: The CO<sub>2</sub> anomaly (using only coincidental observations). Third panel: The percentage difference between SCIAMACHY and the mean aircraft CO<sub>2</sub> mixing ratio (over all altitudes).

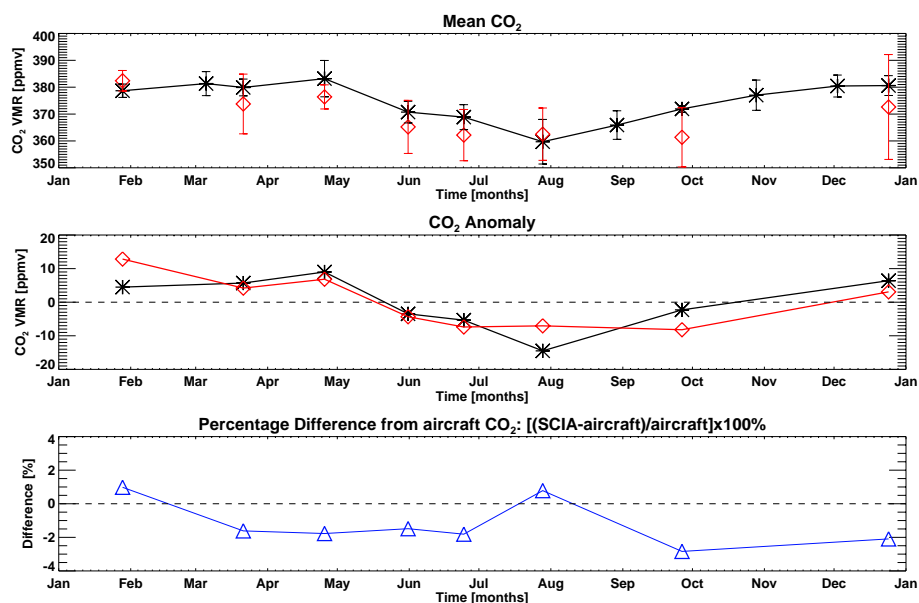


**Fig. 6.** As Fig. 5 but for the CO<sub>2</sub> time series over Novosibirsk.

### 5.3.2 North America

Further to the study outlined in Sect. 5.3.1, a comparison between two consecutive years (2003–2004) of SCIAMACHY CO<sub>2</sub> measurements to WDCGG surface data over North America was also conducted. Whilst there are numerous operational sampling stations in North America, only four

locations (within the USA) were deemed suitable for this assessment. These sites were selected on the basis of having the most number of collocated retrievals to give a more complete time series of SCIAMACHY observations. Owing to the much larger scene observed, as compared to Western Europe, the collocation limits were expanded to  $\pm 5.0^\circ$  latitude and  $\pm 5.0^\circ$  longitude of each location.

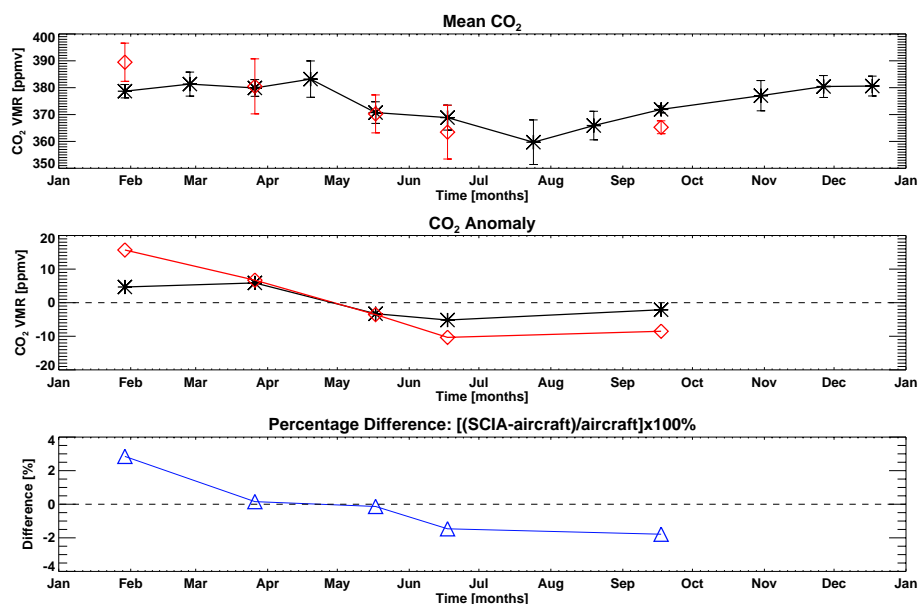


Fig. 7. As Fig. 5 but for the CO<sub>2</sub> time series over Sargut.

Of the four sites considered, Niwot Ridge, despite its high altitude, yields the best agreement to SCIAMACHY with a correlation coefficient of 0.91 and a similar seasonal cycle amplitude of  $\sim 9$  ppmv (Table 4 and Fig. 12). The phasing between the two observed seasonal cycles is also very similar. However, at this location the a priori closely follows the surface measurements. Similarly, at Wendover the correlation between SCIAMACHY and the surface observations is high and seasonal amplitudes comparable but again the a priori and surface signals are much alike. At Park Falls and Point Arena the agreement is worse. In spite of this, the observations made at Park Falls are important as they demonstrate that SCIAMACHY detects a seasonal signal that is more similar to the surface observations than the a priori (this is also evident for the Park Falls tower measurements shown in Fig. 13). As the surface albedo tends to be higher at Niwot Ridge and Wendover, than at Park Falls, the signal to noise ratio of the SCIAMACHY measurements is better and the FSI retrievals more accurate at these locations. Thus, it is more likely that observed SCIAMACHY signals at Niwot Ridge and Wendover are realistic and not simply the case that the retrievals are following the a priori. The poor match at Point Arena is most likely to arise from its coastal location and the constraint that only SCIAMACHY observations over land are considered.

To complement these comparisons, tower data taken from the NOAA/ESRL network and the Sylvania tower, in Michigan, was also evaluated against SCIAMACHY CO<sub>2</sub>. Each tower measures the CO<sub>2</sub> volume mixing ratio at several different heights with a sampling interval, ranging from minutes to hourly, differing between individual sites (see e.g. Bakwin

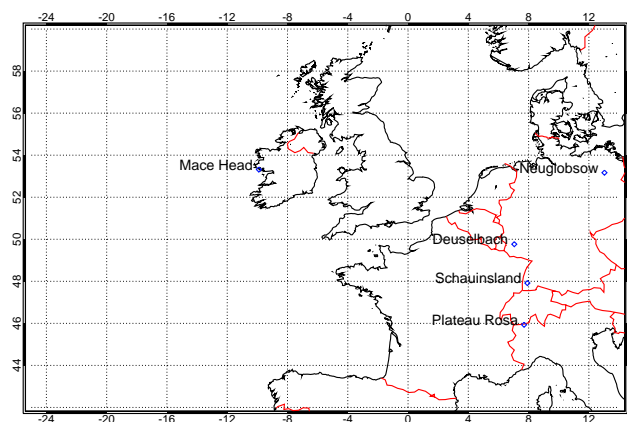
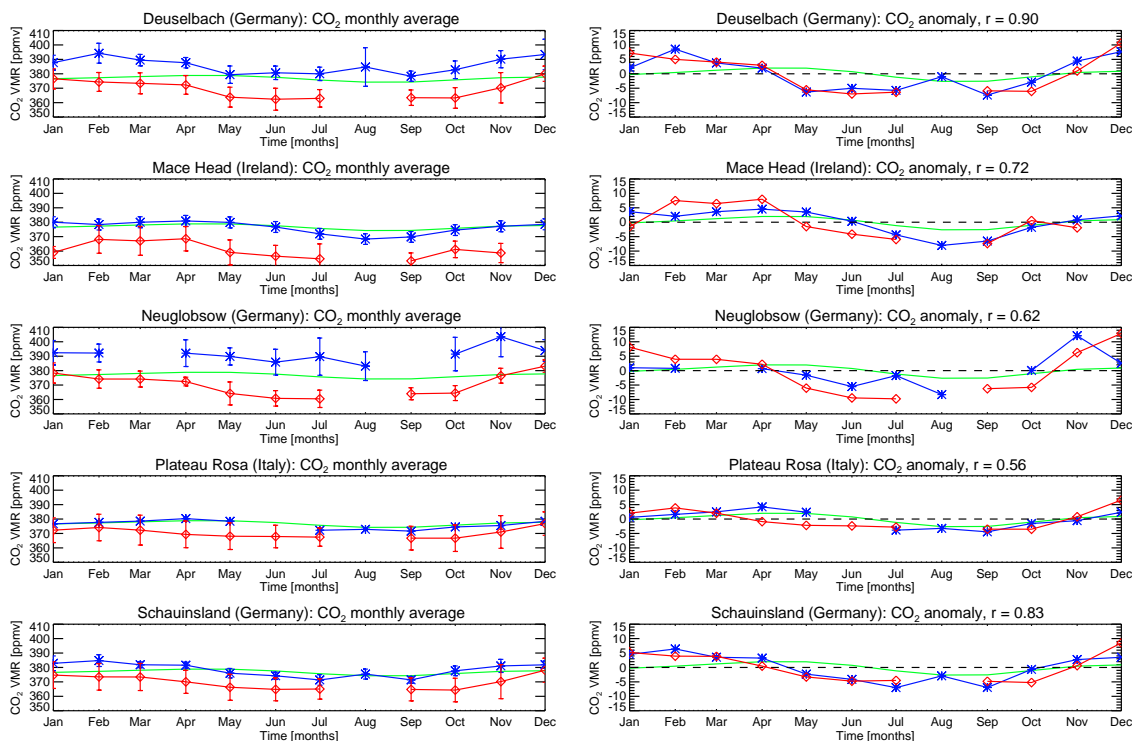
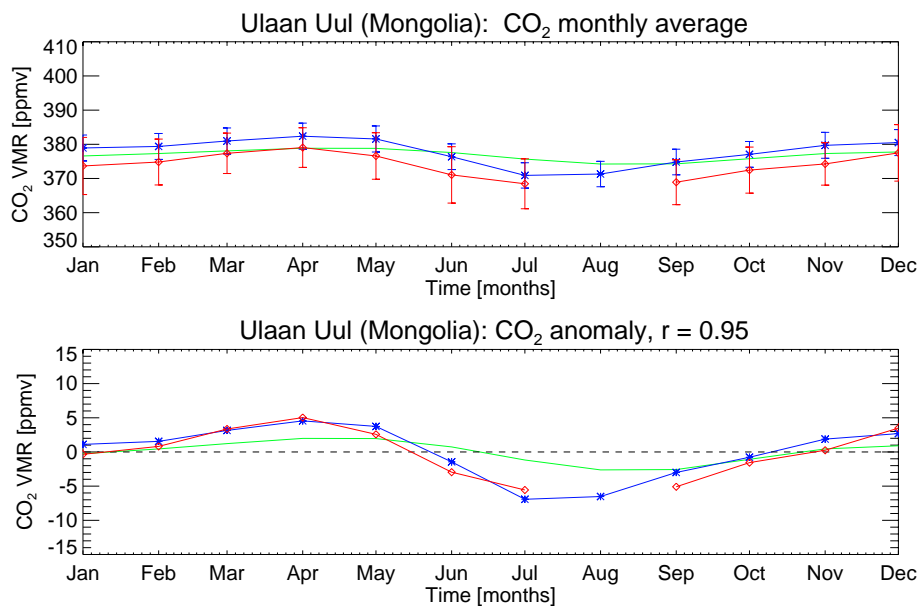


Fig. 8. The surface stations located within the European scene processed by the FSI retrieval algorithm.

and Tans, 1995, or Desai et al., 2005). For each tower, CO<sub>2</sub> volume mixing ratio was averaged over all the intake heights and then assembled into a monthly mean time series. The only exception was the Sylvania tower, where the maximum intake height (36 m) was used instead. The resultant time series were then compared to SCIAMACHY observations using the same collocation limits as for the surface measurements. With the exception of Park Falls, where the correlation is 0.92, the agreement between SCIAMACHY and the tower measurements is not noteworthy. This is irrespective of the fact that the magnitude of seasonal cycle amplitudes are very similar (bar the tower at Argyle where a SCIAMACHY outlier in December distorts the amplitude). At Park Falls



**Fig. 9.** Time series of ground based European in situ observations (blue) versus SCIAMACHY CO<sub>2</sub> (red). The 1 $\sigma$  error bars are shown on the monthly averages. The a priori CO<sub>2</sub> column VMR is shown in green.



**Fig. 10.** As Fig. 9 but for Ulaan Uul, Mongolia.

however, SCIAMACHY agrees with the tower data much better than with the CO<sub>2</sub> measurements made at the surface. For example, there is especially good agreement in the summer months of 2004 where the changes in the mean CO<sub>2</sub> vol-

ume mixing ratios are captured well by SCIAMACHY. The strong correlation is most likely a consequence of the fact that the Park Falls tower measurements can be representative of the entire (well-mixed) PBL (Bakwin and Tans, 1995). At

the Sylvania tower, which is quite close to Park Falls, the correlation is not as strong owing to a slight phase difference relative to the time series of SCIAMACHY observations and possibly also because of the low CO<sub>2</sub> intake height. The incomplete tower time series at Argyle coupled with the sites proximity to the eastern coast contribute to the poor correlation with the time series observed by SCIAMACHY.

#### 5.4 Summary

Evaluating the FSI CO<sub>2</sub> retrievals against the ground based observations, demonstrates that the column variability observed by SCIAMACHY, is similar to changes in surface CO<sub>2</sub> concentrations. Out of the seventeen time series comparisons (including those of the aircraft), eleven have correlation coefficients of 0.7 or greater and moreover comparable seasonal cycle amplitudes. At locations where the agreement to SCIAMACHY is poor, mitigating circumstances such as high site altitude or proximity to the coast, or scene edge, are the probable cause. Whilst the simulations in Sect. 5.1 suggest that SCIAMACHY should see a seasonal signal smaller than that at the surface, observations indicate otherwise. It could be possible that SCIAMACHY is simply over estimating the seasonal cycle, owing to some problem with the retrieval itself. Additionally, at Niwot Ridge and Wendover the a priori is similar to the seasonal signal that SCIAMACHY detects, which might indicate that the retrievals are biased from the input data. However, the phasing and changes in the CO<sub>2</sub> anomalies, for example at Deuselbach or the Park Falls tower where smooth seasonal cycles do not occur, match that well that this cannot be the case. Furthermore, it must be remembered that the same a priori CO<sub>2</sub> data has been used in the SCIAMACHY retrievals at all these locations. Thus, the good agreement at Ullann Uul, Deuselbach and Niwot Ridge, which have very different seasonal signals, cannot all be attributed to the a priori. Hence, it is therefore clear that SCIAMACHY is apparently sensitive to the lower troposphere and that surface data can be used as a useful validation proxy for satellite column measurements when considering only variations in the monthly CO<sub>2</sub> means rather than absolute magnitudes.

## 6 Case study: North America

### 6.1 Spatial distributions

The two years of SCIAMACHY data processed by the FSI algorithm over North America allows the inter-annual variability of the retrieved CO<sub>2</sub> spatial distributions to be examined (Figs. 14 and 15). Despite using a different set of a priori data (i.e. 2004 ECMWF fields and a 2004 CO<sub>2</sub> climatology, instead of 2003 data) within the algorithm, there are quite startling coincidences between monthly scenes of each year. For example, in both years during April a thin band of high CO<sub>2</sub> VMRs is witnessed at high latitudes over

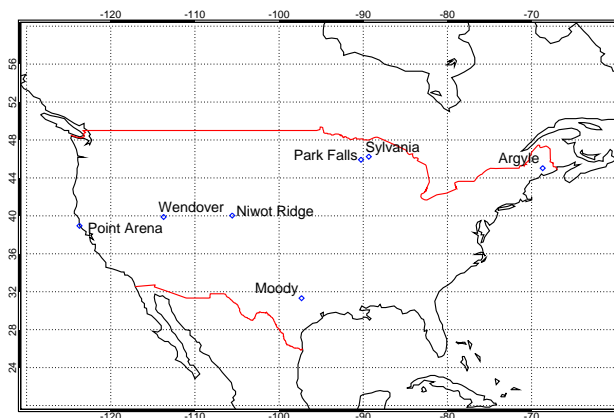


**Fig. 11.** The sampling locations over the USA for (a) surface sites: Niwot Ridge (40.03° N, 105.56° W, surface altitude = 3526 m), Point Arena (38.95° N, 123.72° W, 17 m) and Wendover (39.88° N, 113.717° W, 1320 m) and (b) tower sites: Argyle (45.03° N, 68.68° W, surface altitude = 157 m, maximum intake height = 107 m), Sylvania Tower (46.24° N, 89.34° W, 500 m, 36 m) and Moody Tower (31.32° N, 97.33° W, 256 m, 457 m). At Park Falls (45.92° N, 90.27° W, 868 m, 396.0 m) both surface and tower CO<sub>2</sub> measurements were available.

Ellesmere Island whilst the position of a small localized enhancement over Wyoming (approximately 45° N, 107° E) in 2003, is in the same location as a much more widespread enhancement in 2004. During May, there are low CO<sub>2</sub> VMRs observed over the Appalachian Mountains and southern eastern states in both 2003 and 2004. By July of each year, this feature develops into significant band of very low CO<sub>2</sub> along the eastern U.S. and also up along the Canadian Shield (though to a lesser extent in 2004). In September, as vegetation photosynthesis is weakening, the CO<sub>2</sub> distributions are much more uniform although there are localized regions of low VMRs e.g. along the Newfoundland Coast or over the Saskatchewan Province in (central) Canada. During October and November, of both years, the retrieved CO<sub>2</sub> fields are again very uniform.

The regional patterns within the 2003–2004 North America CO<sub>2</sub> distributions raises several questions. For instance, are these features real, i.e. do the distributions contain the signature of surface fluxes? Can the CO<sub>2</sub> enhancements and depletions be related to surface processes such as CO<sub>2</sub> emissions or photosynthetic activity, or are they simply a residual surface albedo effect?

There are two arguments for eliminating a possible dominant (seasonal) surface reflectance bias. Firstly, an a priori albedo, determined from the mean radiance of each individual SCIAMACHY observation, is used within the FSI algorithm to generate each reference spectrum. A comparison of the monthly gridded a priori surface albedo (not shown) to the retrieved CO<sub>2</sub> VMRs reveals that whilst the CO<sub>2</sub> distributions evolve considerably with time the a priori albedo shows

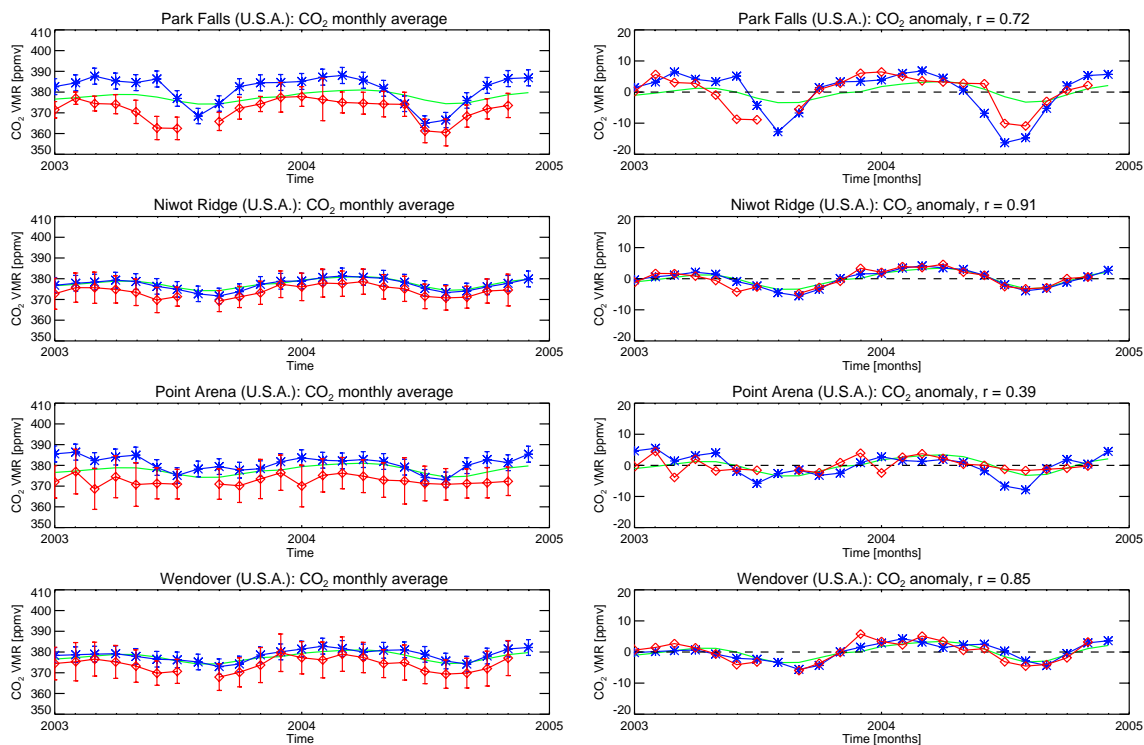


**Fig. 12.** As Fig. 9 but for the U.S. surface in situ observations (blue) versus SCIAMACHY CO<sub>2</sub> (red) over the USA.

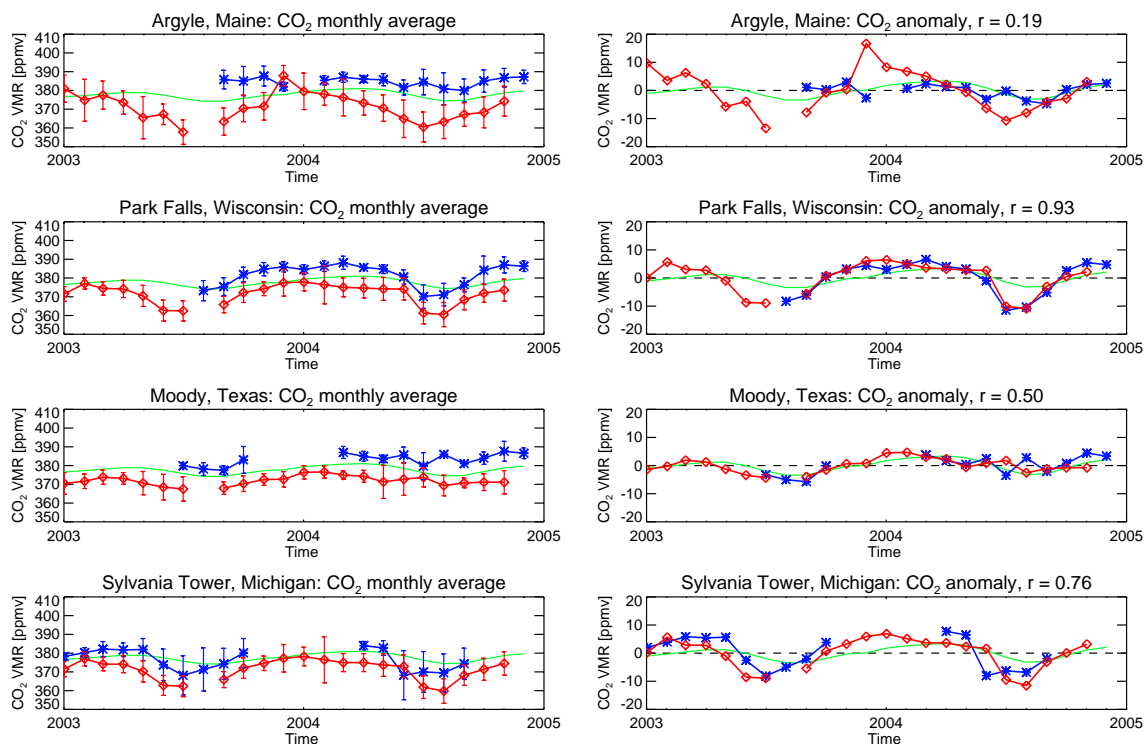


**Fig. 13.** As Fig. 9 but for the U.S. tower observations (blue) versus SCIAMACHY CO<sub>2</sub> (red).

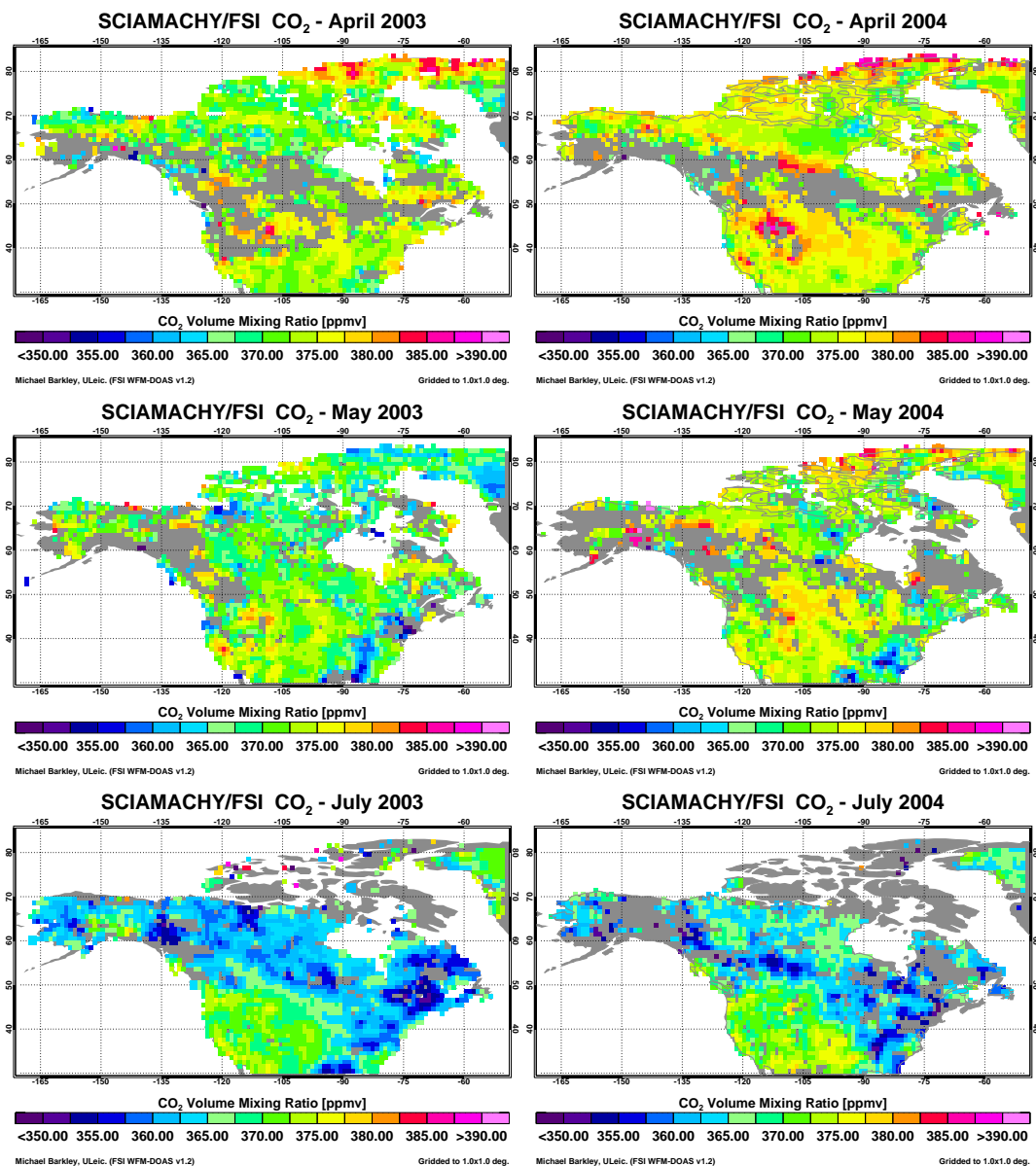


**Fig. 14.** SCIAMACHY observations over North America for April, May and July 2003 (left panels) and 2004 (right panels). All retrievals have been gridded to  $1^\circ \times 1^\circ$  and smoothed with a  $3^\circ \times 3^\circ$  box car average.

little variation. Secondly, the comparison between AIRS and SCIAMACHY performed by Barkley et al. (2006b) demonstrated that over North America both instruments essentially observe the same large scale features. With AIRS being a thermal IR instrument, the surface albedo has negligible effect on the data, thus the CO<sub>2</sub> variability most likely arises from changes in its atmospheric concentration. If SCIAMACHY observes the same features, when accounting for surface reflectance within the retrieval, then it too must be observing the same fluctuations in the column integral.

## 6.2 Correlation with vegetation type

In this section the correlation between the spatial distribution of SCIAMACHY CO<sub>2</sub> and land vegetation cover is explored by comparing SCIAMACHY measurements to five different indicators of vegetation activity at twenty-four different locations in the USA (listed in Table 5). The vegetation proxies were taken from the MODerate resolution Imaging Spectroradiometer (MODIS) ASCII subset products<sup>3</sup> which are extracted from the global land products for a  $7 \text{ km} \times 7 \text{ km}$  area

<sup>3</sup>Downloadable from <http://www.modis.ornl.gov/modis/index.cfm>.

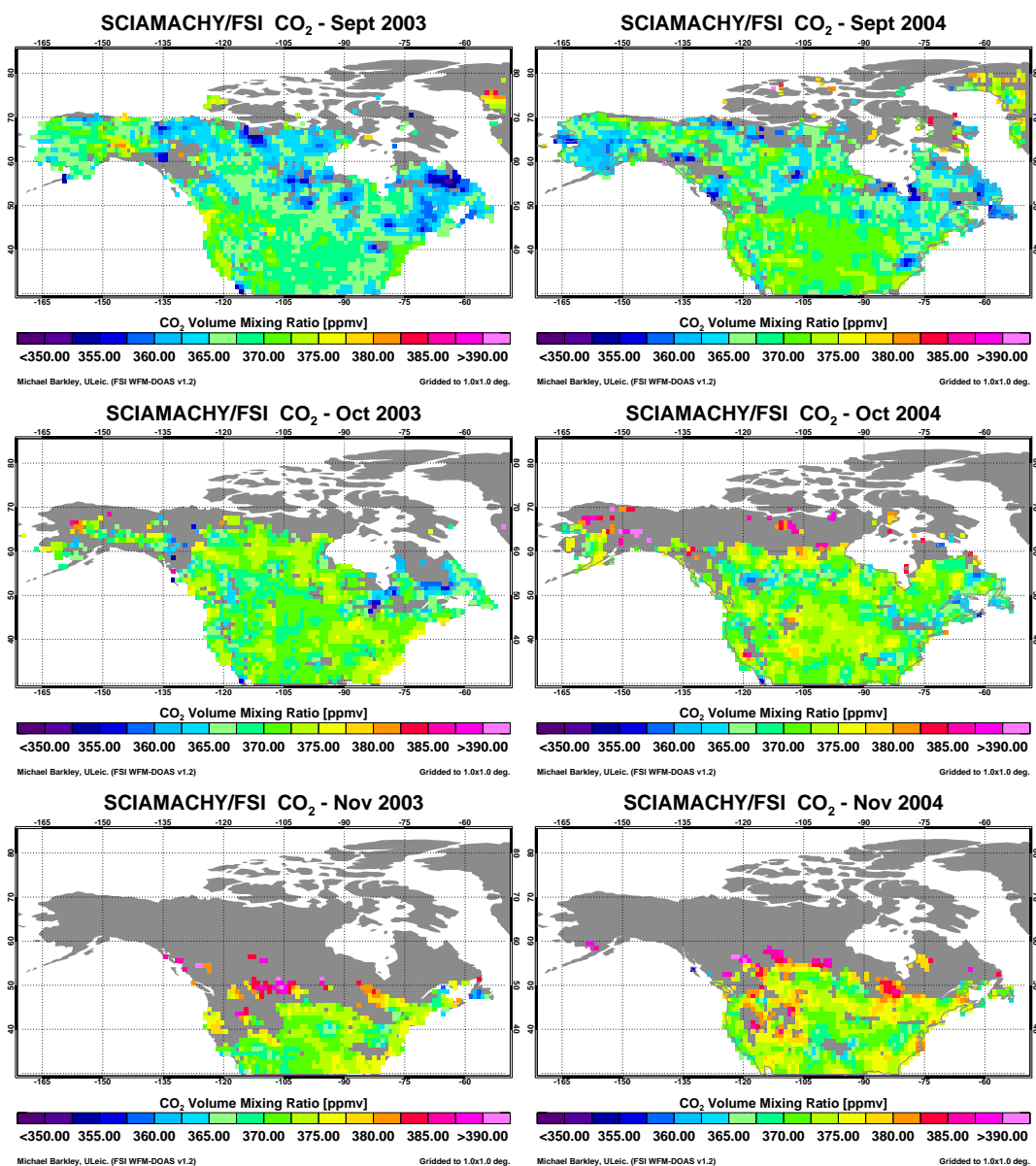


Fig. 15. As Fig. 14 but for September, October and November 2003–2004.

centred on selected flux towers or field sites located around the world. The MODIS instrument measures light in 36 spectral channels (non-continuously) over a wavelength interval of 0.4–14.4  $\mu\text{m}$ . Two channels are imaged at a nominal ground resolution of 250 m at nadir, five channels at 500 m and the other 29 bands at 1 km. The instrument's mirror has a  $\pm 55^\circ$  scanning pattern which yields a swath of 2330 km (cross track) by 10 km (along track at nadir). Global coverage is achieved every one to two days. The MODIS vegetation data used in this comparison are:

– *Normalized Difference Vegetation Index (NDVI)*

Vegetation is a strong absorber of visible radiation, except for green light ( $\lambda=510\text{ nm}$ ), which is in contrast to

NIR radiation which is mostly reflected and scattered by the canopy foliage. The Normalized Difference Vegetation Index (NDVI) is a chlorophyll sensitive index that uses a normalized ratio, between the red and NIR wavelengths, to determine both the presence and condition of vegetation within a satellite footprint:

$$\text{NDVI} = \frac{\rho_{\text{NIR}} - \rho_{\text{red}}}{\rho_{\text{NIR}} + \rho_{\text{red}}} \quad (4)$$

where  $\rho_{\text{red}}$  and  $\rho_{\text{NIR}}$  are the surface bidirectional reflectance factors of the respective MODIS red and NIR bands (Huete et al., 1999). Whilst the NDVI has widely used for operational monitoring (see Huete et al. (2002)

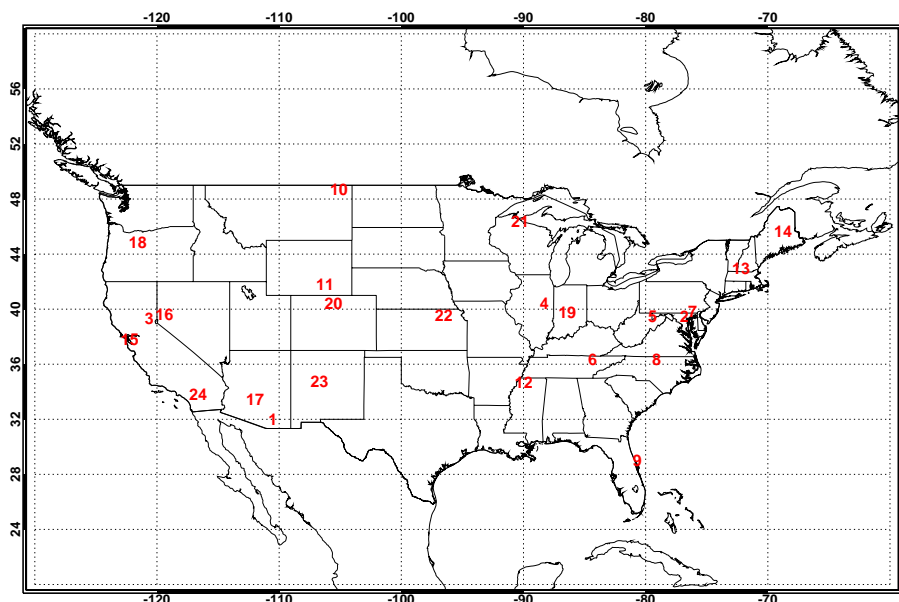


**Fig. 16.** The locations used in the SCIAMACHY/MODIS comparison (see Table 5): 1. Audubon Research Ranch, Arizona, 2. Beltsville Agricultural Research Center, Maryland, 3. Blodgett Forest, California, 4. Bondville, Illinois, 5. Canaan Valley, West Virginia, 6. Chestnut Ridge, Oak Ridge, Tennessee, 7. Cub Hill (Baltimore), Maryland, 8. Duke Forest – loblolly pine, North Carolina, 9. Florida-Kennedy Space Center (scrub oak), 10. Fort Peck, Montana, 11. GLEES, Wyoming, 12. Goodwin Creek, Mississippi, 13. Harvard Forest EMS Tower, Massachusetts, 14. Howland Forest (west tower), Maine, 15. Jasper Ridge, California, 16. Lake Tahoe, Nevada, 17. Maricopa Agricultural Center, Arizona, 18. Metolius-intermediate aged ponderosa pine, Oregon, 19. Morgan Monroe State Forest, Indiana, 20. Niwot Ridge Forest, Colorado, 21. Park Falls/WLEF, Wisconsin, 22. Rannells Ranch (ungrazed), Kansas, 23. Sevilleta BigFoot, New Mexico and 24. Sky Oaks, Young Stand, California.

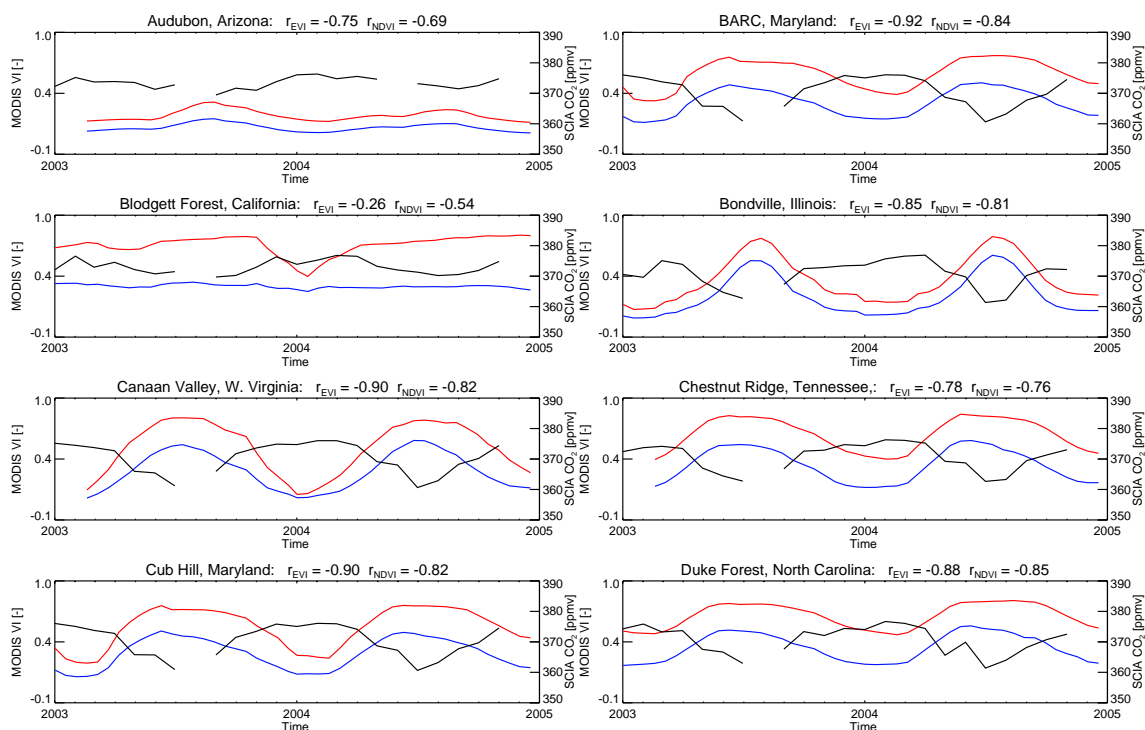


**Fig. 17.** SCIAMACHY CO<sub>2</sub> (black line) plotted against MODIS NDVI (red line) and EVI (blue line) data, at sites 1–8 within the U.S. (see Table 5 and Fig. 16) for the time period 2003–2004. Both the NDVI and EVI data were scaled by 0.0001.

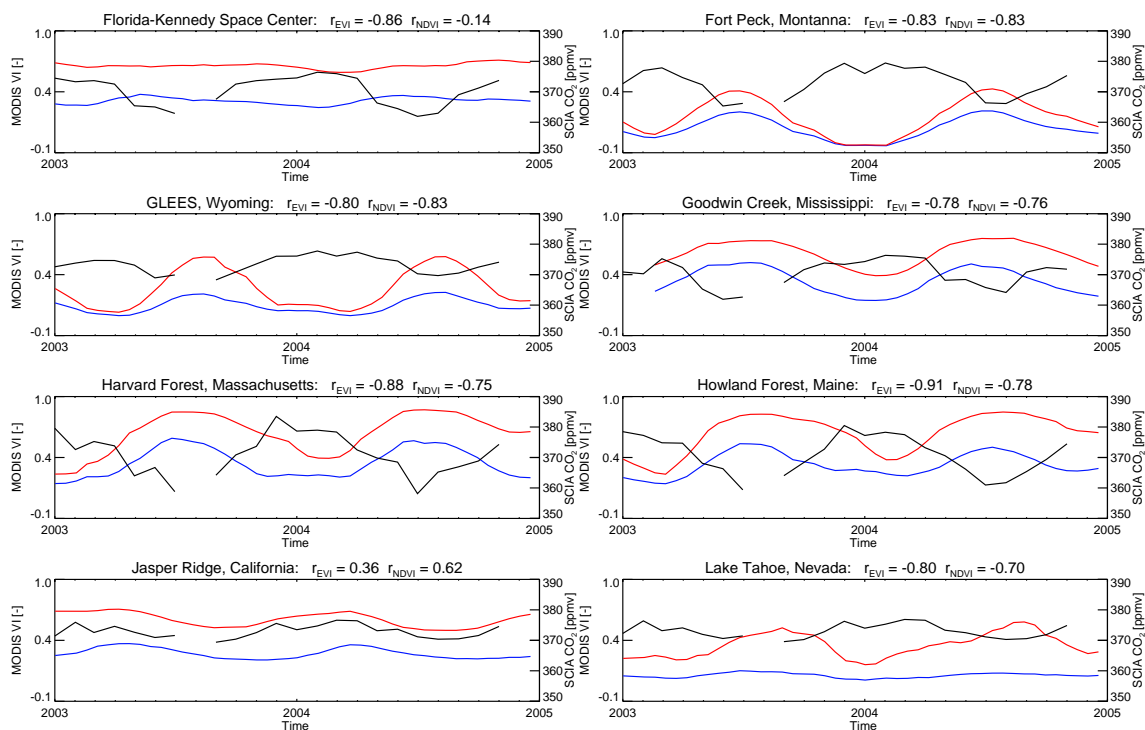


**Fig. 18.** As Fig. 17 but at sites 9–16 within the U.S. (see Table 5 and Fig. 16).

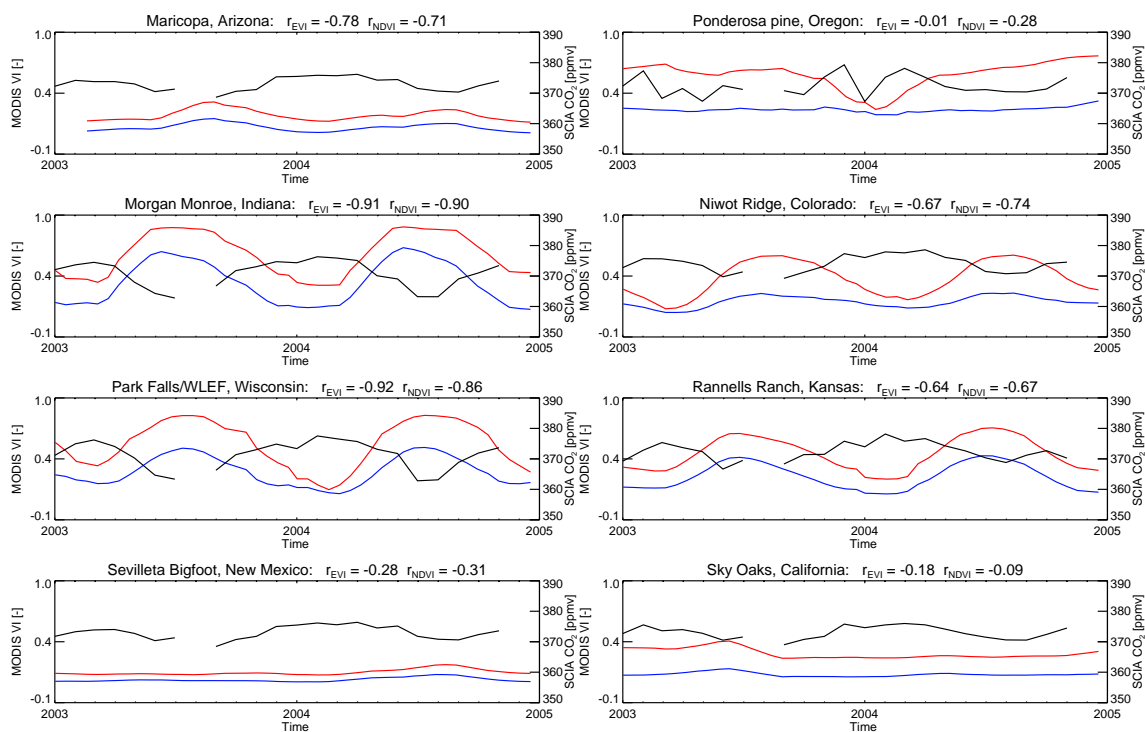


**Fig. 19.** As Fig. 17 but at sites 17–24 within the U.S. (see Table 5 and Fig. 16).

**Table 5.** Summary of the comparison between SCIAMACHY and MODIS vegetation indices data. The correlations are between the SCIAMACHY CO<sub>2</sub> monthly averages and the (time interpolated) MODIS index. The vegetation type is taken from the MODIS MOD12Q1 Land Cover product.

Site Index/Name	Vegetation Type	Correlation				
		EVI	NDVI	FPAR	LAI	GPP
1. Audubon Research Ranch, Arizona, USA	Desert/grassland	-0.75	-0.69	-0.72	-0.72	-0.53
2. Beltsville Agricultural Research Center, Maryland	Deciduous broadleaf	-0.92	-0.84	-0.77	-0.91	-0.51
3. Blodgett Forest, California	Evergreen needleleaf forest	-0.26	-0.54	-0.39	-0.36	-0.31
4. Bondville, Illinois	Croplands	-0.85	-0.81	-0.77	-0.74	-0.48
5. Canaan Valley, West Virginia	Cropland/natural mosaic	-0.90	-0.82	-0.84	-0.93	-0.53
6. Chestnut Ridge, Oak Ridge, Tennessee	Deciduous broadleaf	-0.78	-0.76	-0.76	-0.87	-0.50
7. Cub Hill (Baltimore), Maryland	Urban	-0.90	-0.82	-0.75	-0.86	-0.52
8. Duke Forest - loblolly pine, North Carolina	Mixed forests	-0.88	-0.85	-0.68	-0.89	-0.37
9. Florida-Kennedy Space Center (scrub oak)	Evergreen needleleaf forest	-0.86	-0.14	-0.20	-0.80	-0.36
10. Fort Peck, Montana	Grasslands	-0.83	-0.83	-0.36	-0.07	-0.57
11. GLEES, Wyoming	Woody savannas	-0.80	-0.83	-0.79	-0.78	-0.65
12. Goodwin Creek, Mississippi	Cropland/natural mosaic	-0.78	-0.76	-0.85	-0.87	-0.58
13. Harvard Forest EMS Tower, Massachusetts (HFR1)	Mixed forests	-0.88	-0.75	-0.75	-0.83	-0.52
14. Howland Forest (west tower), Maine	Mixed forests	-0.91	-0.78	-0.80	-0.92	-0.51
15. Jasper Ridge, California	Woody savannas	0.36	0.62	0.11	0.32	-0.33
16. Lake Tahoe, Nevada	Woody savannas	-0.80	-0.70	-0.77	-0.79	-0.54
17. Maricopa Agricultural Center, Arizona	Grasslands	-0.78	-0.71	-0.25	-0.43	0.10
18. Metolius-intermediate aged ponderosa pine, Oregon	Evergreen needle leaf forests	-0.01	-0.28	-0.25	-0.27	-0.29
19. Morgan Monroe State Forest, Indiana	Deciduous broadleaf	-0.91	-0.90	-0.81	-0.88	-0.52
20. Niwot Ridge Forest, Colorado (LTER NWT1)	Evergreen needleleaf forests	-0.67	-0.74	-0.71	-0.72	-0.65
21. Park Falls/WLEF, Wisconsin	Woody savannas	-0.92	-0.86	-0.81	-0.92	-0.58
22. Rannells Ranch (ungrazed), Kansas	Grasslands	-0.64	-0.67	-0.63	-0.54	-0.51
23. Sevilleta BigFoot, New Mexico	Grasslands	-0.28	-0.31	-0.45	-0.48	-0.56
24. Sky Oaks, Young Stand, California	Closed shrubland	-0.18	-0.09	-0.35	-0.34	-0.23

and references therein) and provides a long term (20+ year) indicator of vegetation activity it can suffer from atmospheric contamination (e.g. aerosols), saturation over areas of high biomass and is sensitive to variations in the canopy background (Huete et al., 2002). The NDVI product used in this analysis is from the MOD13A2 product which is 16-day composite at 1 km resolution.

#### – Enhanced Vegetation Index (EVI)

The EVI was developed to counter the problematic effects of the NDVI by normalizing the reflectance in the red band by that in the blue band:

$$EVI = G \times \frac{\rho_{NIR} - \rho_{red}}{\rho_{NIR} + (C_1 \times \rho_{red} - C_2 \times \rho_{blue}) + L} \quad (5)$$

where  $\rho_{red}$ ,  $\rho_{NIR}$  and  $\rho_{blue}$  are the atmospherically corrected surface reflectances,  $L$  is the canopy background adjustment (to account for radiative transfer through the canopy),  $G$  is a gain term ( $\sim 2.5$ ) and  $C_1$  and  $C_2$  are coefficients to correct for the presence of aerosols (Huete et al., 1999).

The advantage of the EVI, compared to the NDVI, is that is more sensitive to the canopy structure rather than chlorophyll content. The EVI is less affected therefore from atmospheric and canopy background contamination and has increased sensitivity (i.e. less saturation) at high biomass levels. The EVI is also taken from the MOD13A2 product.

#### – The Fraction of Photosynthetically Absorbed Radiation (FPAR)

FPAR is a measure of the fraction of available radiation, in photosynthetically active wavelengths (400 to 700 nm), that a vegetation canopy absorbs. FPAR is derived (by the MODIS algorithm) from the atmospherically corrected surface reflectance using coupled atmospheric and surface radiative transfer models (Knyazikhin et al., 1999). The FPAR data is taken from the MOD15A2 product which is at 1 km spatial resolution and over an 8-day period.

#### – Leaf Area Index (LAI)

LAI, also taken from the MOD15A2 product, is a biophysical parameter that describes the structure of the

vegetation canopy and is defined as one sided leaf area per unit ground area (Knyazikhin et al., 1999):

$$\text{LAI} = \frac{1}{X_s \cdot Y_s} \int_V u_L(r) dr \quad (6)$$

where  $V$  is the canopy domain in which a given plant is located,  $X_s$  and  $Y_s$  are the horizontal dimensions of  $V$  and  $u_L(r)$  is a 3-D leaf area distribution function which describes the heterogeneity of the canopy. The LAI is derived using complex radiative transfer models and is non-linearly related to the FPAR.

#### – Gross Primary Production (GPP)

The GPP, expressed as the mass of carbon per square metre, can be estimated in very simplistic terms, by multiplying FPAR by the amount of photosynthetically active radiation (PAR) and then by a conversion efficiency factor  $\varepsilon$  which represents how much radiation is converted in to plant biomass (Running et al., 1999). The GPP data is taken from the MOD17A2 data and is a composite over an 8-day period.

The ground sites were chosen, out of the complete network, to give widespread geographical coverage and also to incorporate a wide variety of land cover types (see Fig. 16 and Table 5). Each vegetation proxy was smoothed with a 5 point moving average and plotted against the corresponding SCIAMACHY time series, constructed from taking the mean of all monthly gridded CO<sub>2</sub> data lying within  $\pm 5.0^\circ$  latitude and  $\pm 5.0^\circ$  longitude of each site. Although these collocation limits for SCIAMACHY are much greater than 7 km  $\times$  7 km boundaries for MODIS, it is necessary to ensure a smoother and more complete CO<sub>2</sub> time series. For NDVI, EVI, FPAR and LAI this comparison was performed over a two year time period (2003–2004) whereas for the GPP product only data for 2003 was available.

Examinations of the time series plots (e.g. Figs. 17–19) reveal that there is a strong anti correlation between the retrieved CO<sub>2</sub> VMRs and each of the vegetation proxies. That is, as the terrestrial biosphere becomes more active, as photosynthesis starts to dominate over respiration, atmospheric CO<sub>2</sub> tends to a minimum in the summer months. This is in contrast to the vegetation proxies which peak in summer, owing to the vegetation's response to more light and warmer temperatures. Hence, there is a six month phase difference between CO<sub>2</sub> and the vegetation proxies.

Of the vegetation indices, there is slightly better correlation with the EVI than NDVI, with the strongest agreement at BARC (Maryland), Morgan Monroe State Forest, Park Falls and Howland Forest. These sites are covered by deciduous broadleaf or mixed forests and woody savannas, which have a strong seasonal CO<sub>2</sub> signal. The lowest correlations occur at Shy Oaks (closed shrubland), Sevilleta BigFoot (grasslands) and Jasper Ridge (woody savannas) where there is a

lack of dense vegetation. This draws attention to the fact that where the the vegetation index (VI, i.e. EVI or NDVI) is high the retrieved CO<sub>2</sub> variability is also large, for example at Canaan Valley or Bondville (Table 5). If there is a weak CO<sub>2</sub> seasonal cycle then the variability of the VIs is also small. This is evident at Audubon, Maricopa or any of the locations where the correlation was low. Plotting the amplitude of the CO<sub>2</sub> seasonal cycle measured by SCIAMACHY against the respective seasonal amplitudes of the VIs (Fig. 20) illustrates this well as there are not any low VI/high CO<sub>2</sub> or high VI/low CO<sub>2</sub> combinations. The correlation between the SCIAMACHY CO<sub>2</sub> and the NDVI and EVI seasonal amplitudes are significant at 0.56 and 0.68, respectively.

Very similar trends are found for the time series of FPAR and LAI (not shown) with the best correlations with SCIAMACHY CO<sub>2</sub> occurring at Canaan Valley, Goodwin Creek, Morgan Monroe State Forest and Park Falls and the worst at Shy Oaks, Sevilleta BigFoot and Jasper Ridge (i.e. in the same corresponding locations as the VI correlations). The variability of FPAR and LAI is also closely linked to the CO<sub>2</sub> variability. This is evident at Shy Oaks and Sevilleta where there is minimal seasonal variability in CO<sub>2</sub> or either proxy. That aside, the correlation of the FPAR and LAI seasonal amplitudes against the retrieved CO<sub>2</sub> signal is worse than as found for the VIs, being 0.25 and 0.30, respectively (Fig. 20).

The correlation for each between the MODIS GPP and SCIAMACHY CO<sub>2</sub> time series (not shown) are very similar, typically 0.3–0.5. These correlations are noticeably lower than those between SCIAMACHY CO<sub>2</sub> and NDVI, EVI, FPAR or LAI. For the GPP, the best correlations occur at Niwot Ridge and GLEES, Wyoming, whereas the worst are at Mircopa, Arizona (positive correlation) and Shy Oaks. The correlation between the GPP seasonal amplitude and CO<sub>2</sub> is also significant at 0.59.

From this preliminary comparison it can therefore be concluded that SCIAMACHY CO<sub>2</sub> correlates reasonably with the terrestrial biosphere, with low vegetation activity equating to low CO<sub>2</sub> variability. For a more complete analysis, climatological variables such as temperature and precipitation which affect plant growth, also need to be included. However, greater sampling by SCIAMACHY and improvements to FSI retrievals are needed to reduce the collocation limits before such a more detailed point analysis can be undertaken. Nevertheless this study is encouraging since it indicates the potential for combining SCIAMACHY atmospheric data and MODIS land products in the future to help investigate the behaviour of the terrestrial biosphere.

## 7 Conclusions

One of the major issues regarding the retrieval of atmospheric CO<sub>2</sub> from space is the subject of near surface sensitivity. In this paper, SCIAMACHY CO<sub>2</sub> retrieved using the FSI algorithm has been compared to a variety of in situ

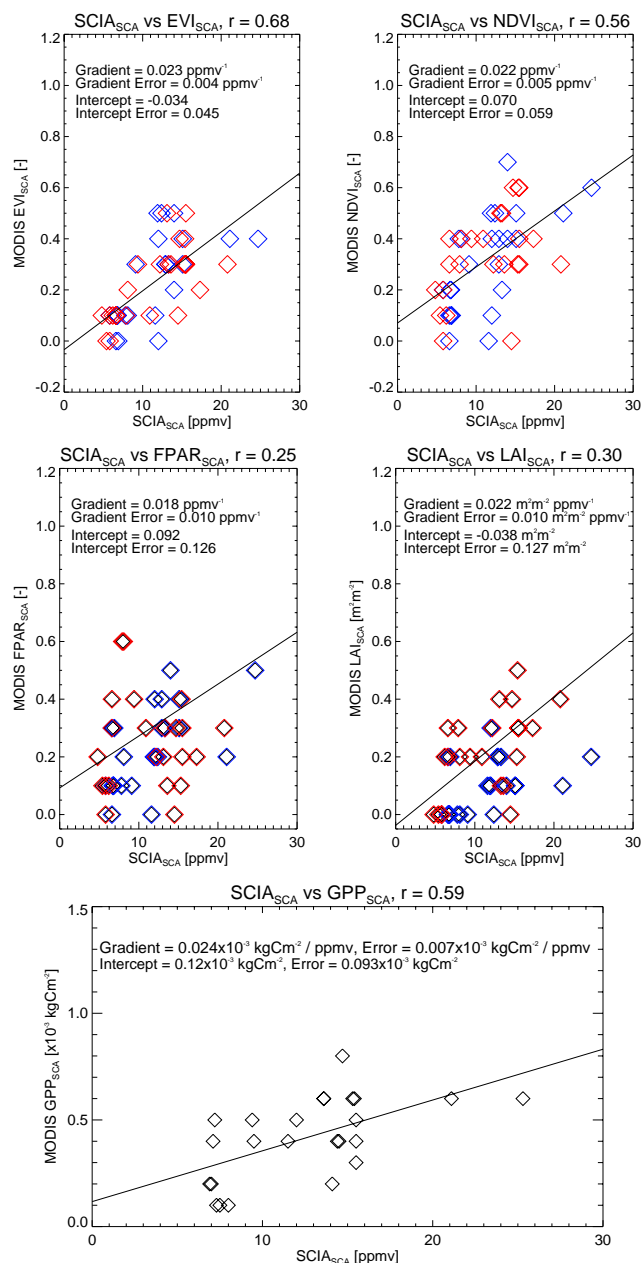


**Fig. 20.** Plots of the MODIS vegetation proxy seasonal cycle amplitudes against those of SCIAMACHY's CO<sub>2</sub> separated into the years 2003 (blue) and 2004 (red).

CO<sub>2</sub> measurements to assess the instrument's sensitivity to the lower troposphere and planetary boundary layer. Initial validation, of the daily average CO<sub>2</sub> VMR, against FTS column measurements made at Park Falls, Wisconsin, during 2004 reveal a negative bias of approximately -2% when using SCIAMACHY observations lying within  $\pm 1^\circ$  longitude and latitude of the site. However, this bias becomes smaller if the collocation criteria is relaxed as more SCIAMACHY observations can be used in the calculation of the

daily mean. The collocation limits selected also affect the ability of SCIAMACHY to detect day to day variability. As the collocation limits are expanded then the daily variability is captured better, whereas if they are reduced, monthly timescales must be considered instead.

The comparisons to the aircraft measurements over Siberia and to the surface and tower measurements demonstrate that SCIAMACHY is capable of observing a seasonal cycle that is consistent with the seasonal signal of lower tropospheric and surface CO<sub>2</sub>. Whilst there is always a negative offset to the absolute magnitudes, the monthly anomalies of SCIAMACHY and the surface stations often agree well and are not believed to be biased by the input a priori CO<sub>2</sub> data. When discrepancies do occur, poor sampling around the site is the most attributable cause.

Additional evidence of the near surface sensitivity of SCIAMACHY is demonstrated by the significant correlations with the MODIS vegetation indices, that are representative of terrestrial vegetation activity over the selected U.S. locations. At many sites, low (or high) vegetation activity is often allied to correspondingly to low (or high) CO<sub>2</sub> variability. As the seasonal variability of vegetation affects the surface reflectance, SCIAMACHY CO<sub>2</sub> retrievals might be biased by vegetation activity. However, the comparison between SCIAMACHY and AIRS CO<sub>2</sub> over North America by Barkley et al. (2006b), indicated that the SCIAMACHY retrievals are not biased by the seasonal variation in surface albedo. Hence, SCIAMACHY has the potential ability to observe variations in CO<sub>2</sub> that arise from terrestrial vegetation activity i.e. to detect surface CO<sub>2</sub> fluxes. However, as the validation against the FTS measurements at Park Falls demonstrated, improvements to the FSI retrieval algorithm must be made to remove any negative biases and to improve the precision of the CO<sub>2</sub> observations to more firmly establish the capability of SCIAMACHY for surface flux detection.

*Acknowledgements.* The authors would like to thank all those involved with the SCIAMACHY instrument especially J. Burrows and the team at IUP/IFE Bremen. We are also grateful to A. Rozanov for supplying the radiative transfer model SCIATRAN. We would like to thank ESA and SRON for supplying the SCIAMACHY data and additionally R. van Hees (of SRON). Thanks also to R. Washenfelder, G. Aleks, G. Toon, and P. Wennberg at Caltech and NASA JPL for the provision of the Park Falls FTS measurements which were obtained with support from NASA. We also are grateful to British Atmospheric Data Centre (BADC) for supplying the ECMWF operational data set. Furthermore, the authors would collectively like to thank all the data providers at each CO<sub>2</sub> sampling station and their respective funding partners and both the NOAA/ESRL and WDCGG networks. The authors finally wish to thank the Natural Environment Research Council (NERC) and CASIX (the Centre for observation of Air-Sea Interactions and fluxes) for supporting M. Barkley through grant ref: NER/S/D/200311751 and NERC and the Data Assimilation Research Council (DARC) for supporting A. Hewitt through grant ref: NER/S/A/2005/13330.

Edited by: W. E. Asher

## References

- Bakwin, P. S. and Tans, P. P.: Measurements of carbon dioxide on a very tall tower, *Tellus*, 47B, 535–549, 1995.
- Barkley, M. P., Frieß, U., and Monks, P. S.: Measuring atmospheric CO<sub>2</sub> from space using Full Spectral Initiation (FSI) WFM-DOAS, *Atmos. Chem. Phys.*, 6, 3517–3534, 2006a.
- Barkley, M. P., Monks, P. S., and Engelen, R. J.: Comparison of SCIAMACHY and AIRS CO<sub>2</sub> measurements over North America during the summer and autumn of 2003, *Geophys. Res. Lett.*, 33, L20805, doi:10.1029/2006GL026807, 2006b.
- Barkley, M. P., Monks, P. S., Frieß, U., Mittermeier, R. L., Fast, H., Körner, S., and Heimann, M.: Comparisons between SCIAMACHY atmospheric CO<sub>2</sub> retrieved using (FSI) WFM-DOAS to ground based FTIR data and the TM3 chemistry transport model, *Atmos. Chem. Phys.*, 6, 4483–4498, 2006c.
- Bösch, H., Toon, G. C., Sen, B., Washenfelder, R., Wennberg, P. O., Buchwitz, M., de Beek, R., Burrows, J. P., Crisp, D., Christi, M., Connor, B. J., Natraj, V., and Yung, Y. L.: Space-based Near-Infrared CO<sub>2</sub> Retrievals: Testing the OCO Retrieval and Validation Concept Using SCIAMACHY Measurements over Park Falls, Wisconsin, *J. Geophys. Res.*, 111, D23302, doi:10.1029/2006JD007080, 2006.
- Bovensmann, H., Burrows, J. P., Buchwitz, M., Frerick, J., Noël, S., Rozanov, V. V., Chance, K. V., and Goede, A.: SCIAMACHY – mission objectives and measurement modes, *J. Atmos. Sci.*, 56, 127–150, 1999.
- Buchwitz, M., Rozanov, V. V., and Burrows, J. P.: A near infrared optimized DOAS method for the fast global retrieval of atmospheric CH<sub>4</sub>, CO, CO<sub>2</sub>, H<sub>2</sub>O, and N<sub>2</sub>O total column amounts from SCIAMACHY/ENVISAT-1 nadir radiances, *J. Geophys. Res.*, 105, 15 231–15 246, 2000.
- Buchwitz, M., de Beek, R., Burrows, J. P., Bovensmann, H., Warneke, T., Notholt, J., Meirink, J. F., Goede, A. P. H., Bergamaschi, P., Körner, S., Heimann, M., and Schulz, A.: Atmospheric methane and carbon dioxide from SCIAMACHY satellite data: initial comparison with chemistry and transport models, *Atmos. Chem. Phys.*, 5, 941–962, 2005a.
- Buchwitz, M., de Beek, R., Noël, S., Burrows, J. P., Bovensmann, H., Bremer, H., Bergamaschi, P., Körner, S., and Heimann, M.: Carbon monoxide, methane and carbon dioxide columns retrieved from SCIAMACHY by WFM-DOAS: year 2003 initial data set, *Atmos. Chem. Phys.*, 5, 3313–3329, 2005b.
- Buchwitz, M., de Beek, R., Noël, S., Burrows, J. P., Bovensmann, H., Schneising, O., Khlystova, I., Bruns, M., Bremer, H., Bergamaschi, P., Körner, S., and Heimann, M.: Atmospheric carbon gases retrieved from SCIAMACHY by WFM-DOAS: version 0.5 CO and CH<sub>4</sub> and impact of calibration improvements on CO<sub>2</sub> retrieval, *Atmos. Chem. Phys.*, 6, 2727–2751, 2006, <http://www.atmos-chem-phys.net/6/2727/2006/>.
- Desai, A. R., Bolstad, P., Cook, B. D., Davis, K. J., and Carey, E. V.: Comparing net ecosystem exchange of carbon dioxide between an old-growth and mature forest in the upper MidWest, USA, *Agric. Forest Meteorol.*, 128, 33–35, 2005.
- Dils, B., De Mazière, M., Müller, J. F., Blumenstock, T., Buchwitz, M., de Beek, R., Demoulin, P., Duchatelet, P., Fast, H., Frankenberg, C., Gloudemans, A., Griffith, D., Jones, N., Kerzenmacher, T., Kramer, I., Mahieu, E., Mellqvist, J., Mittermeier, R. L., Notholt, J., Rinsland, C. P., Schrijver, H., Smale, D., Strandberg, A., Straume, A. G., Stremme, W., Strong, K., Sussmann, R., Taylor, J., van den Broek, M., Velasco, V., Wagner, T., Warneke, T., Wiacek, A., and Wood, S.: Comparisons between SCIAMACHY and ground-based FTIR data for total columns of CO, CH<sub>4</sub>, CO<sub>2</sub> and N<sub>2</sub>O, *Atmos. Chem. Phys.*, 6, 1953–1976, 2006, <http://www.atmos-chem-phys.net/6/1953/2006/>.
- Engelen, R. J. and McNally, A. P.: Estimating atmospheric CO<sub>2</sub> from advanced infrared satellite radiances within an operational four-dimensional variational (4D-Var) data assimilation system: Results and validation, *J. Geophys. Res.*, 110, D18305, doi:10.1029/2005JD005982, 2005.
- Gloudemans, A. M. S., Schrijver, H., Kleipool, Q., van den Broek, M. M. P., Straume, A. G., Lichtenberg, G., van Hees, R., Aben, I., and Meirink, J. F.: The impact of SCIAMACHY near-infrared instrument calibration on CH<sub>4</sub> and CO total columns, *Atmos. Chem. Phys.*, 5, 2369–2383, 2005, <http://www.atmos-chem-phys.net/5/2369/2005/>.
- Gottwald, M., Bovensmann, H., Lichtenberg, G., Noël, S., von Barmen, A., Slijkhuis, S., Piters, A., Hoogeveen, R., von Savigny, C., Buchwitz, M., Kokhanovsky, A., Richter, A., Rozanov, A., Holzer-Popp, T., Bramstedt, K., Lambert, J.-C., Skupin, J., Wittrock, F., Schrijver, and Burrows, J. P.: SCIAMACHY Monitoring the Earth's Changing Atmosphere, DLR, Institut für Methodik der Fernerkundung (IMF), Germany, 2006.
- Gurney, K. R., Law, R. M., Denning, A. S., Rayner, P. J., Baker, D., Bousquet, P., Bruhwiler, L., Chen, Y.-H., Ciais, P., Fan, S., Fung, I. Y., Gloor, M., Heimann, M., Higuchi, K., John, J., Maki, T., Maksyutov, S., Masariek, K., Peylin, P., Prather, M., Pak, B. C., Randerson, J., Sarmiento, J., Taguchi, S., Takahashi, T., and Yuen, C.-W.: Towards robust regional estimates of sources and sinks using atmospheric transport models, *Nature*, 415, 626–630, 2002.
- Houweling, S., Bréon, F.-M., Aben, I., Rödenbeck, C., Gloor, M., Heimann, M., and Ciais, P.: Inverse modeling of CO<sub>2</sub> sources and sinks using satellite data: a synthetic inter-comparison of measurement techniques and their performance as a function of space and time, *Atmos. Chem. Phys.*, 4, 523–538, 2004, <http://www.atmos-chem-phys.net/4/523/2004/>.
- Houweling, S., Hartmann, W., Aben, I., Schrijver, H., Skidmore, J., Roelofs, G.-J., and Bréon, F.-M.: Evidence of systematic errors in SCIAMACHY-observed CO<sub>2</sub> due to aerosols, *Atmos. Chem. Phys.*, 5, 3003–3013, 2005, <http://www.atmos-chem-phys.net/5/3003/2005/>.
- Huete, A., Justice, C., and van Leeuwen, W.: MODIS Vegetation Index (MOD 13) Algorithm Theoretical Basis Document, 1999.
- Huete, A., Didan, K., Miura, T., Rodriguez, E. P., Gao, X., and Ferreira, L. G.: Overview of the radiometric and biophysical performance of the MODIS vegetation indices, *Remote Sens. Environ.*, 83, 195–213, 2002.
- Kiehl, J. T. and Trenberth, K. E.: Earth's Annual Global Mean Energy Budget, *Bulletin of the American Meteorological Society*, 78, 197–208, 1997.
- Kleipool, Q.: Algorithm Specification for Dark Signal Determination, Tech. rep., SRON-SCIA-30 PhE-RP-009, SRON, 2003a.
- Kleipool, Q.: Recalculation of OPTEC5 Non-Linearity, Report containing the NL correction to be implemented in the data proces-

- sor, Tech. rep. SRON-SCIA-PhE-RP-013, SRON, 2003b.
- Kneizys, F. X., Abreu, L. W., Anderson, G. P., Shettle, E. P., Chetwynd, J. H., Shettle, E. P., Berk, A., Bernstein, L., Robertson, D., Acharya, P., Rothman, L., Selby, J. E. A., Allery, W. O., and Clough, S. A.: The MODTRAN 2/3 report and LOWTRAN 7 model, Tech. rep., Philips Laboratory, Hanscom AFB, 1996.
- Knyazikhin, Y., Glassy, J., Privette, J. L., Tian, Y., Lotsch, A., Zhang, Y., Wang, Y., Morisette, J. T., Votava, P., Myneni, R. B., and Nemani, S. W. R.: MODIS Leaf Area Index (LAI) And Fraction Of Photosynthetically Active Radiation Absorbed By Vegetation (FPAR) Product (MOD15) Algorithm Theoretical Basis Document Version 4.0, 1999.
- Krijger, J. M., Aben, I., and Schrijver, H.: Distinction between clouds and ice/snow covered surfaces in the identification of cloud-free observations using SCIAMACHY PMDs, *Atmos. Chem. Phys.*, 5, 2279–2738, 2005, <http://www.atmos-chem-phys.net/5/2279/2005/>.
- Machida, T., Nakazawa, T., Muksyutov, S., Tohjima, Y., Takahashi, Y., Watai, T., Vinnichenko, N., Panchenko, M., Arshinov, M., Fedoseev, N., and Inoue, G.: Temporal and spatial variations of atmospheric CO<sub>2</sub> mixing ratio over Siberia, *Proceedings of The Sixth International CO<sub>2</sub> Conference*, Sendai, Japan, 2001.
- Miller, C. E., Crisp, D., DeCola, P. L., Olsen, S. C., Randerson, J. T., Michalak, A. M., Alkhaled, A., Rayner, P., Jacob, D. J., Suntharalingam, P., Jones, D. B. A., Denning, A. S., Nicholls, M. E., Doney, S. C., Pawson, S., Boesch, H., Connor, B. J., Fung, I. Y., O'Brien, D., Salawitch, R. J., Sander, S. P., Sen, B., Tans, P., Toon, G. C., Wennberg, P. O., Wofsy, S. C., Yung, L., and Law, R. M.: Precision requirements for space-based X<sub>CO<sub>2</sub></sub> data, *J. Geophys. Res.*, 112, D10314, doi:10.1029/2006JD007659, 2007.
- O'Brien, D. M. and Rayner, P. J.: Global observations of the carbon budget, 2. CO<sub>2</sub> column from differential absorption of reflected sunlight in the 1.61 μm band of CO<sub>2</sub>, *J. Geophys. Res.*, 107, D14354, doi:10.1029/2001JD000617, 2002.
- Patra, P. K., Gurney, K. R., Denning, A. S., Maksyutov, S., Nakazawa, T., Baker, D., Bousquet, P., Bruhwiler, L., Chen, Y.-H., Ciais, P., Fan, S., Fung, I., Gloor, M., Heimann, M., Higuchi, K., John, J., Law, R. M., Maki, T., Pak, B. C., Peylin, P., Prather, M., Rayner, P. J., Sarmiento, J., Taguchi, S., Takahashi, T., and Yuen, C.-W.: Sensitivity of inverse estimation of annual mean CO<sub>2</sub> sources and sinks to ocean-only sites versus all-sites observational networks, *Geophys. Res. Lett.*, 33, L05814, doi:10.1029/2005GL025403, 2006.
- Remedios, J. J., Parker, R. J., Panchal, M., Leigh, R. J., and Corlett, G.: Signatures of atmospheric and surface climate variables through analyses of infrared spectra (SATSCAN-IR), *Proceedings of the first EPS/METOP RAO Workshop*, ESRIN, 2006.
- Rödenbeck, C., Houweling, S., Gloor, M., and Heimann, M.: CO<sub>2</sub> flux history 1982–2001 inferred from atmospheric data using a global inversion of atmospheric transport, *Atmos. Chem. Phys.*, 3, 1919–1964, 2003, <http://www.atmos-chem-phys.net/3/1919/2003/>.
- Rothman, L., Jacquemart, D., Barbe, A., Benner, C. D., Birk, M., Brown, L. R., Carleer, M. R., Chackerian Jr., C., Chance, K., Coudert, L. H., Dana, V., Devi, V. M., Flaud, J.-M., Gamache, R. R., Goldman, A., Hartmann, J.-M., Jucks, J. W., Maki, A. G., Mandin, J.-Y., Massie, S. T., Orphal, J., Perrin, A., Rinsland, C. P., Smith, M., Tennyson, J., Tolchenov, R. N., Toth, R. A., Vander Auwera, J., Varanasi, P., and Wagner, G.: The HITRAN 2004 molecular spectroscopic database, *J. Quant. Spectrosc. Radiat. Transfer*, 96, 193–204, 2005.
- Rozañov, V. V., Buchwitz, M., Eichmann, K. U., de Beek, R., and Burrows, J. P.: SCIAMACHY – a new radiative transfer model for geophysical applications in the 240–2400 nm spectral region: The pseudo-spherical version, presented at COSPAR 2000, *Adv. Space Res.*, 29(11), 1831–1835, 2002.
- Running, S. W., Nemani, R., Glassy, J. M., and Thornton, P. E.: MODIS Daily Photosynthesis (PSN) and annual Net Primary Production (NPP)(MOD17) Algorithm Theoretical Basis Document, 1999.
- Siegenthaler, U., Stocker, T. F., Monnin, E., Lüthi, D., Schwander, J., Stauffer, B., Raynaud, D., Barnola, J.-M., Fischer, H., and Valérie Masson-Delmotte, J. J.: Stable Carbon Cycle-Climate Relationship During the Late Pleistocene, *Science*, 310, 1313–1317, 2005.
- Tiwari, Y. K., Gloor, M., Engelen, R. J., Chevallier, F., Rödenbeck, C., Körner, S., Peylin, P., Braswell, B. H., and Heimann, M.: Comparing CO<sub>2</sub> retrieved from AIRS with model predictions: implications for constraining surface fluxes and lower-troposphere transport, *J. Geophys. Res.*, 111, D17106, doi:10.1029/2005JD006681, 2006.
- Washenfelder, R. A., Toon, G. C., Yang, Z., Allen, N. T., Wennberg, P. O., Vay, S. A., Matross, D. M., and Daube, B. C.: Carbon dioxide column abundances at the Wisconsin Tall Tower site, *J. Geophys. Res.*, 111, D22305, doi:10.1029/2006JD007154, 2006.